

ENGINEERING PROVISION TO CONTROL THE STATE OF FISSION INDUCED BY THERMAL EFFECTS-CASE STUDY BAWANUR DAM

Prof. Dr. Univ. Ing. Stematiu Dan.

By PhD Student Objed Wissam.

Technical University of civil engineering of Bucharest

Contents

Chapter 1: Introduction	3
Background information	3
The objective of the Study	4
Research Needs	4
Literature Review	4
Introduction	4
Controlling mass concrete temperatures	5
Allowable temperature difference	6
Chapter 2: THERMAL ANALYSIS	7
Introduction	7
Transient Thermal Analysis	7
Heat of Hydration	8
Thermal Gradients	9
Thermal diffusivity	9
Thermal conductivity	10
Specific heat capacity	11
Density	11
Pipe cooling	11
Chapter 3: Case Study (BAWANUR DAM)	12
Introduction	12
DESIGNED DAM PARAMETERS	13
Finite element method	16
Introduction	16
ANSYS Finite Element Modeling	17
THERMAL PROPERTIES	17
SOLID 70 Element Description	19
Boundary Conditions	19
ANSYS Finite Element spillway of BAWANUR DAM	22
MASS CONCRETE BLOCK EXPERIMENT (Lawrence 2009)	26
Introduction	26
Block Geometry	27
Instrumentation for Data Collection Introduction	28

Model Geometry30Chapter 4: FINITE ELEMENT ANALYSIS RESULTS31Thermal Analysis Results31Structure Analysis Results34Overview of Finite Element Structural Model34Material Model34Modulus of Elasticity34Poisson's Ratio35Coefficient of Thermal Expansion35Stress Results36Conclusion41References43	Temperature Profiles	29
Thermal Analysis Results	Model Geometry	30
Structure Analysis Results	Chapter 4: FINITE ELEMENT ANALYSIS RESULTS	31
Overview of Finite Element Structural Model 34 Material Model 34 Modulus of Elasticity 34 Poisson's Ratio 35 Coefficient of Thermal Expansion 35 Stress Results 36 Conclusion 41	Thermal Analysis Results	31
Material Model 34 Modulus of Elasticity 34 Poisson's Ratio 35 Coefficient of Thermal Expansion 35 Stress Results 36 Conclusion 41	Structure Analysis Results	34
Modulus of Elasticity	Overview of Finite Element Structural Model	34
Poisson's Ratio	Material Model	34
Coefficient of Thermal Expansion	Modulus of Elasticity	34
Stress Results	Poisson's Ratio	35
Conclusion41	Coefficient of Thermal Expansion	35
	Stress Results	36
References	Conclusion	41
	References	43

Chapter 1: Introduction

Background information

Modern concrete technology allows contractors to produce high-performance concrete with high cement content to increase the rate of strength gain to reduce formwork removal time for accelerated construction schedules. Consequently, concrete placements with an increased amount of cement contents result in higher peak temperatures, as well as temperature differentials between the concrete surface and the interior. The hydration of concrete is an exothermic process producing a significant amount of heat within concrete elements. When the heat of hydration slows down, the surface of concrete tends to cool down much faster than the inside. Therefore, tensile stresses occur from the restraining volume of concrete which can result in thermal cracking at an early age. At the same time, higher curing temperatures will speed up the hydration process and the concrete matures faster at an early age. This concept was introduced to the concrete industry as a maturity concept to predict concrete strength development in terms of temperature and time by monitoring the in-place concrete temperatures in realtime (Saul 1951). To reduce the temperature differentials, and thus prevent cracking in mass concrete, some of the common methods such as precooling of concrete, post-cooling of concrete with cooling pipes, and insulation or insulated formwork should be used. (Tia, Ferraro et al. 2010). Currently, common practices attempt to control concrete thermal cracking by controlling the temperatures within the concrete. This is primarily done through four methods: modification of the concrete mix design, precooling of mixed materials, post-cooling of in-place concrete, and surface insulation. The goal of these practices is to reduce the maximum internal temperature achieved as well as to control the rate at which heat dissipates, thus controlling the temperature gradients. These specifications, however, vary from state to state, with agreement only on the typical maximum temperature differential limit of 35 °F. Concrete hydration is an exothermic reaction that can produce high amounts of heat during curing, especially in the first few days or weeks after casting. In large volumes of concrete, known as mass concrete, this heat production can produce high temperatures at the center of the concrete's mass due to the insulating effect of the concrete. When the concrete surface temperatures are lower due to the heat dissipated into the ambient environment, temperature gradients are formed. These changes in temperature create volumetric changes, expansion from heating and contraction from cooling, in the concrete. The collapse of WTC towers provided an impetus for structural _reengineering research and development in many research organizations worldwide. However, it is recognized that the implementation of performancebased approaches requires several key elements that are currently not fully developed or understood (Law, Stern-Gottfried et al. 2011, Kodur, Garlock et al. 2012).

The objective of the Study

The goal of the research is to develop a finite element model of mass concrete (BAWANUR DAM sample), which is based on the input of measured thermal and mechanical characteristics, Develop a temperature control model from the combined work of other researchers and which can predict the temperature distribution during hydration and the thermal stresses that result from the thermal gradients within the structure. Previous attempts at predicting the temperature.

Research Needs

The high amount of heat that develops during the hydration of massive concrete structures produces very high temperatures throughout the structure. The maximum allowable temperature differential shall be limited to 35°F (20°C) and the maximum allowable concrete temperature shall be limited to 160°F (70°C). This research investigates the thermal performance and cracking risk of mass concrete and develops a finite element model of mass concrete in ANSYS APDL Program.

Literature Review

Introduction

According to the ACI, mass concrete is defined as "any volume of concrete with dimensions large enough to require that measures be taken to cope with generation of heat from the hydration of cement and attendant volume change to minimize cracking" (R-07 2007). In addition to that, ACI Committee 301 presents an optional requirement checklist to assist the engineers in selecting and specifying project requirements in the specification. Roughly, mass concrete is defined by a minimum dimension of 2.5 feet (0.75 m) or a minimum cement content of 600 pounds per cubic yard (350kg/m3) (ACI Committee 301, 2005). Portland Cement Association (PCA) describes mass concrete as any concrete placement with a minimum dimension of 36 inches (915 mm), or concrete batched with a minimum of 600 pounds per cubic yard (350 kg/m3) TYPE III or high-early-strength cement regardless its dimension that could cause high internal temperatures exceeding 158°F (70°C). Additionally, concrete placements should be considered as mass concrete where thermal cracking may occur due to high-temperature differentials between the center and the surface of the structure (Gajda 2007). Nowadays, any concrete placement that leads to thermal cracking is considered as mass concrete regardless of its dimensions. Therefore, estimation of thermal behavior has become necessary to minimize or eliminate cracking of concrete due to thermal issues in order to ensure long term durability for extended service life of the concrete structures.

This chapter presents a review of available literature on the principles of heat transfer and explains how these principles can be used to manage the thermal behavior of concrete dams. Assyrian and Babylonian civilizations were among the earliest recorded users of clay as the binding material in ancient times. In 1756, John Smeaton is credited with the creation of the first modern concrete which he achieved by adding pebbles as a coarse aggregate and mixing powered brick into the cement. This was the earliest discovery of the benefits of limestone as a cementation binder (White 1977). In 1824, Joseph Aspdin invented Portland cement, which has remained the principal binder used in concrete production, although in present times cement composition is chemically far different. Aspdin created the first artificial cement by burning ground limestone and clay together at high temperatures. This burning process modified the chemical properties of the materials, resulting in stronger cement than that which plain crushed limestone would generate (Ghosh 1991). The ultimate goal of assembling this information is to implement it in the proposed temperature control model. The temperature in mass concrete structures has an important effect on dam construction schedule and safety. The main factor contributing to temperature rise in mass concrete is heat evolution due to an exothermic reaction of cement. Understanding the mechanism of heat generation for cement is the key to controlling the temperature of mass concrete. Thermal analysis of massive concrete structures is a common topic in many massive concrete publications. In most of those publications, the focus is the thermal load caused by the heat of hydration of cement, in other words, thermal studies of young concrete. The most suitable numerical methods for the current application are considered to be the finite difference and finite element methods. The finite element method is preferred over the finite difference method, mainly because

- i. the finite element method has greater flexibility in terms of the geometries that can be evaluated and
- ii. That commercial finite element analysis software packages for transient temperature analysis are more widely available. As the technique that is used to solve the heat flow equation greatly affects the results obtained, the use of the finite element method to solve the heat flow equation is evaluated in terms of its ability to accurately model transient concrete temperature profiles.

Controlling mass concrete temperatures

Construction practices of how to control mass concrete temperatures vary. Prescriptive specifications with simplistic methods have been found effective controlling temperatures to minimize cracking in mass concrete placements. These methods include limiting maximum cementations content (600 pounds per cubic yard), incorporating fly ash (25%-30%), limiting initial concrete temperatures (75°F-80°F), limiting maximum concrete temperatures (160°C) and temperature differentials (35°C). It requires concrete mix prequalification before placement and temperature monitoring during placement (Committee 2005, R-07 2007)(ACI Committee 207, 2005). ACI recommends using TYPE II or TYPE IV cement or replacing cement with supplementary cementations materials such as

fly ash, ground granulated blast furnace slag (GGBFS) to obtain less heat of hydration. Additionally, decreasing the cement dosage is recommended by ACI to reduce the heat of hydration when 56 or 90-day strength is acceptable for service conditions. Water-curing is also recommended for extra cooling during summertime. Also, pre-cooling the constituent materials, and post-cooling the structure using cooling pipes are suggested in ACI 207.1R for more effective temperature control. Furthermore, ACI suggests preparing a thermal control plan that restricts the temperature differential between the surface and the center of the structure so that thermal cracking can be minimized. When a high maximum concrete temperature is expected, it is recommended to add reinforcement to minimize the crack width. ACI 207.1R provides detailed information about the constituent materials, concrete mixtures, mechanical and thermal properties of inplace concrete, construction methods, and equipment that are necessary for mass concrete applications. Key points about batching, mixing, placing, and curing mass concrete are explained thoroughly. The guideline states that controlling the type and the amount of cementations material is the key to limiting temperature rise inside the concrete (Committee 2005). ACI 207.2R describes typical values for structural properties such as tensile strength and creep, and thermal properties such as specific heat, thermal conductivity, and thermal diffusivity of mass concrete mixtures that can be used to predict cracking potential. The guidelines provide several example problems to estimate initial concrete temperature, temperature rise, and final concrete temperature in mass concrete structures using given charts and tables consisting of empirical data. Schmidt Method for estimating the temperature rise and the differentials were described (ACI Committee 207, 2007). ACI 207.4R summarizes the methodology of different construction procedures that can be used to control temperature development in mass concrete structures. Pre-cooling is one of the most effective methods for reducing the initial concrete temperature. The batch water can be chilled or substituted with ice, and the aggregate piles can be shaded or water-cooled to minimize the fresh concrete temperature. Alternatively, liquid nitrogen can be used to reduce the fresh concrete temperature. Concrete temperatures can be also reduced using post-cooling methods such as embedded water pipe and shading (ACI Committee 207, 2005).

Allowable temperature difference

In mass concrete specifications, the maximum allowable temperature difference is often limited to 35°F (20°C). This limit was proposed by (FitzGibbon and ME 1976). In his study, the cracking strain of concrete was reached when the temperature differential exceeds 35°F (20°C). According to the study, thermal cracking in mass concrete occurs by two different mechanisms, as shown in Figure 2.1. First, thermal cracking occurs because of the instant surface cooling therefore early formwork removal is one of the main reasons for external thermal cracking. Second, thermal cracking occurs when the rate of the surface temperature rise is a lot smaller than the inside during the first day or two after

concrete placement (FitzGibbon and ME 1976)Lately, researchers discuss if the allowable temperature difference of 35°F (20°C) is still viable, since in some cases thermal cracking has not been encountered even at higher temperature difference, and in other cases, cracking was observed when the temperature difference is below 35°F (Gajda 2007)

Chapter 2: THERMAL ANALYSIS

Introduction

The thermal behavior of concrete in its early stage is investigated in this chapter. Although concrete for massive structures like dams has small cement contents, the temperature produced by current hydration becomes extremely high if it is not controlled. The problem analyzed here is transient. Transient thermal analysis is the most common of al thermal analyses. Almost all heat transfer processes are transient. This kind of analysis is used to determine the temperature and other thermal quantities in the body due to different thermal loads. Thermal loads applied to the structure are time-dependent. For practical problems, transient thermal analysis cm is a difficult task, especially when dealing with complicated shapes and long periods. Among different methods of analysis, the finite element method is a very acceptable and commonly used method for such kind of problems. In this particular problem. The commercial finite element program, ANSYS is used. To obtain reliable results, the model should capture the thermal behavior of mass concrete in its early stage. All factors such as changes in model geometry, the heat of hydration of cement, boundary conditions, and the transient incremental procedure must be included.

Transient Thermal Analysis

To make a good simulation of the real model many different factors that can influence the thermal behavior of young concrete have to be included in the algorithms. Some of those factors are concrete block size, placing frequency, change of ambient temperature, the influence of formwork, the heat of hydration as a thermal load, and other factors in the analysis algorithm. As we mentioned earlier, transient thermal processes are common processes in nature. To perform the transient analysis we have to introduce loads that are a function of time. The heat produced by hydration of cement and the change of ambient temperature is two important loads that are dependent on time. Change in ambient temperature is neglected in this analysis. For

Laboratory specimens, this change of temperature does not even exist because the curing process is taking place in a closed area, where the temperature is constant. In the dam model change in the ambient temperature is neglected because the dam model is observed for a small period. Loads From hydration of cement are changed every six hours. For more accurate results, a smaller time step should be

used. However, when a dam model is analyzed the step is increased at the end of the analysis as the effects of initial conditions are no longer important. The first step in a transient analysis is to apply the initial conditions. Usually, the initial conditions are the uniform temperature at all nodes. Later the transient process starts and the thermal field is obtained by solving the classical heat equation. For each time step, the loads as a function of the must are defined.

Heat of Hydration

To properly model the behavior of hydrating concrete, knowledge of the heat produced during the hydration reaction as well as both the material properties of the concrete itself and the environmental conditions in which it is placed are needed.

As previously stated the heat produced during hydration is a function of the temperature history of the concrete. The momentary heat production rate is defined as:-

$$qv(r,T) = \alpha \cdot qr(r) \cdot qT(T) \tag{1}$$

Where:

r = the degree of reaction

T =the temperature $^{\circ}$ C

 α = the maximum value of the heat production rate (J/m³-hr)

 q_r = the degree of reaction dependent heat production (J/m³-hr)

 q_T = the temperature dependent heat production (J/m³-hr)

And,

$$T(T) = e^{\frac{E_a}{R}(r,T)}$$
(2)

In which,

 E_a = the activation energy of the concrete J/mol

 $R = \text{the universal gas constant}, 8.3144 \text{ J/mol-}^{\circ}\text{C}$

The heat production rate which is dependent on degree of reaction, qr, can also be determined by ANSYS using preprocessing. The temperature history produced

under adiabatic hydration conditions is used as the input in this case. ANSYS derives the heat production q (t) from

$$q(t) = c(T, r) \frac{\partial T}{\partial t}$$
(3)

Where: c(T,r) = the capacitance dependent on temperature and degree of reaction

Thermal Gradients

Temperature differences per unit distance along a particular path in a structure are called thermal gradients. These gradients result from the surface of a mass concrete element being cooled by the ambient environment while the internal concrete temperature remains high due to the exothermic reaction of hydration. This causes the surface concrete to be restrained by the interior concrete. This may result in the cracking of the surface concrete. The magnitude of the thermal gradients experienced by concrete depends on the initial placing temperature, the thermal properties (specific heat, thermal conductivity), environmental temperature, and wind speed.

Thermal diffusivity

The first internal factor affecting heat transfer which is considered is thermal diffusivity. Thermal diffusivity is a material-specific parameter that describes how fast temperature changes in the material would occur under a thermal gradient. The thermal diffusivity of a material is dependent on its thermal conductivity, density, and specific heat capacity. While for specific heat there is some fundamental agreement between the various researchers, literature data on the thermal diffusivity of hardening concrete do not seem to be coherent. Constant values during hardening are reported as well as increasing and decreasing tendencies. In 1946, (RILEM and Structures) reported a constant diffusivity for concretes with different compositions. For example, a concrete with 350 kg cement and w/c = 0.5 had a constant thermal diffusivity a = 0.0037 m2/h for ages ranging from 1 to 7 days. (Brown and Javaid 1970) also published test results for the period ranging from 1 to 7 days. For hardening concrete, they found a decrease from 0 -0034 m2/h at 1 day to 0.0029 m2/h at 7 days. (Maréchal 1973) postulated that the thermal diffusivity reaches a maximum at an age of about 50 h. His test results are based on concrete with rapid hardening Portland cement, using a very simple test procedure (see below). Using the same test method, , (Hansen, PF et al. 1982) found an increase of the thermal diffusivity of hardening cement pate from about 0 e 85 to about 1.05 m2/1000 h.

Thermal conductivity

Conduction is the process whereby heat is transmitted through a material when it is subjected to a temperature gradient. Thermal conductivity, simply put, is a basis for comparison of the ability of a material to conduct heat (energy) under a temperature gradient. A volume of concrete with high thermal conductivity will consequently transfer heat (energy) at a greater rate under the same thermal gradient than would be the case for a volume of concrete with low thermal conductivity.

- **Mix proportions**: Concrete is made from ingredients that have dissimilar thermal conductivities. It is clear from various sources that the thermal conductivity of concrete is proportional to the ratio in which the different ingredients are present in the concrete (Choktaweekarn, Saengsoy et al. 2009)
- **Type of aggregate used:** Researchers generally agree that concrete made with aggregate with a lower thermal conductivity will yield concrete with lower conductivity, while the use of more conductive aggregates will yield a more conductive concrete (Khan and Environment 2002)
- **Degree of saturation (moisture content):** The thermal conductivity of air is much lower than that of water. Concrete that is fully saturated will consequently have a higher conductivity (Choktaweekarn, Saengsoy et al. 2009). According to (Khan and Environment 2002) the conductivity of fully saturated concrete is between 44 and 64 % greater than an oven dry sample, depending on the type of aggregate used.
- **Temperature:** Thermal conductivity of concrete decreases nearly linearly with an increase in temperature (Kim, Jeon et al. 2003). However, the effect is small over the range of temperatures that mass concrete is normally exposed to (Ballim and Graham 2009).

Age (degree of hydration): There is disagreement amongst researcher as to the effect of concrete age on thermal conductivity. Some researchers have reported a drop of up to 30 % in thermal conductivity during the first seven days of hydration, while others report no influence at all or a slight increase during the first three to six days (Choktaweekarn, Saengsoy et al. 2009)suggest that the disagreement between the results of the previous researchers can be attributed to the different curing conditions, moisture contents and testing procedures used in these studies.

• **Supplementary cementing materials**: Several authors have shown that replacing a portion of the cementitious content with fly ash reduces concrete's thermal conductivity. The same effect has been observed for blast-furnace slag by (Kim, Jeon et al. 2003).

Specific heat capacity

Specific heat capacity refers to the amount of heat that is required to increase the temperature of a unit mass of a material by 1 °C. The temperature within a volume of concrete with a high specific heat capacity will consequently react slower to a temperature gradient (and internal heat generation) than a volume of concrete with low specific heat capacity.

Density

Density, when viewed in combination with specific heat capacity (density multiplied by specific heat capacity), is a measure of how much heat is required to raise the temperature of a unit volume of material by 1 °C. The temperature of a volume of concrete with a high density will consequently react slower to temperature gradients (or internal heat generation) than a volume of concrete with a low density. The density of concrete is mainly affected by the density of the raw materials it is made from (mass-weighted average), water content, degree of compaction, and air content. The density of mass density commonly ranges between 2240 kg and 2600 kg/m3 according to (Conrad 2006). Table 1 provides a summary of the relative densities of concrete ingredients.

Concrete Ingredient	Relative density	Reference
Cement (CEMI)	3.14	(Addis & Goodman
FLY ASH	2.3	,2009)
Ground granulated blast-	2.9	
furnace slag		

Table 1 Relative densities of cementitious materials commonly.

Pipe cooling

Controlling temperature-induced cracking in concrete is one of the main concerns in the design and construction of concrete dams. The quick construction process and large size of concrete lifts will induce a high temperature or extreme thermal gradient within the concrete and cause significant thermal stresses during the cooling of the dam, which is sufficient for cracking (Zhu and management 1999). Thus, it is necessary to simulate and analyze the temperature and stress fields during construction and then suggest some effective temperature control measures to prevent cracking (Tatro and Schrader 1992). Cooling by the flow of water through an embedded cooling pipe has become a common and effective artificial temperature control measure in the construction of concrete dams, such as in the Hoover Dam. A great deal of research has been conducted to simulate the cooling effect of this water flow. (Cervera, Oliver et al. 2000) presented a numerical procedure for the thermal and stress analysis of the evolutionary construction process of RCC dams. This procedure took into account the ambient

temperature, placing temperature, casting schedule, and, in particular, the more relevant features of the behavior of concrete during the early stages after construction, such as hydration, aging, creep, and damage. The U.S. Bureau of Reclamation (USBR 1949) researched the calculation of the final stage of water cooling and presented an analytical solution using a two-dimensional (2D) program, and an approximate solution using a three-dimensional (3D) program with no heat source by using the separation-of variables method.(Zhu and management 1999) studied the calculation of the initial stage of water cooling and obtained an analytical solution using a 2D program and an approximate solution using a 3D program with a heat source by using the integral transform method. He noted that polythene pipes had fewer joints, which appeared to be more convenient than steel pipes in construction, and he also presented four methods for computing the effect of cooling by nonmetal pipes. Also, he simplified the analysis and proposed methods to compute the equivalent radius and equivalent horizontal spacing of nonmetal pipes. (Zhu and management 1999) treated water cooling as negative hydration heat and presented a cooling equivalent algorithm based on the FEM. He equally distributed the water cooling effect to every element in the FEM analysis, easily obtaining an approximate distribution of the temperature field. This method, which requires only simple programming and exhibits high computational efficiency, has been widely used in recent years. However, this method suffers from oversimplification and cannot accurately reflect the cooling effect, the cooling water velocity, or the temperature variation. (Kim, Jeon et al. 2003) developed a 3D FEM program to thermally analyze concrete structures with pipe cooling systems. Line elements were adapted to model pipes, and internal flow theory was applied during the calculation of the temperature variation of the cooling water

.

Chapter 3: Case Study (BAWANUR DAM)

Introduction

The proposed Bawanur dam is a multipurpose project comprising storage, flood control, irrigation, power production, and recreational uses. Bawanur dam is located on the Sirwan River, which is a left tributary of the Tigris River. The proposed site is located in the northeastern part of Iraq in Källare District - Sulaymaniyah Governorate - Kurdistan Regional Government, near the town of Bawanur Figure (1,2). The Sirwan River originates on the territory of Iran, the catchment area relating to the proposed dam site is 20,142 km2 and Sirwan has the average discharge of water (Qa) approx. 120 m3.s-1. The bottom width of the river valley varies from 600 to 1,200 meters. The dam body is keyed to the right bank near the town of Bawanur and is connected to a public road of local importance. The dam body is designed as an embankment one with clay core.

Stabilization parts of the dam body are designed from local materials – fluvial sand and gravel; the subsoil of the dam is sealed by a secant pile wall made of plastic concrete. The dam appurtenances such as the spillway, bottom outlets, and hydropower station are located at the dam close to the axis of the valley towards the right bank.

The spillway structure is designed as gated, having 6 Tainter gates of a span of 14.0 m and a height of 7.4 m. The total length of the spillway crest is 126 meters. The bottom outlets are linked to spillway construction. They consist of 10 pieces of outlets of a diameter of 3.0 m each, as well as two knife gate valves (emergency and inspection valves) and a Tainter gate as the control gate. The bottom outlets are joined by two concrete tunnels with dimensions of 8.0 x 3.5 m each. The object of the bottom outlet is adjacent to a hydropower station, which will house four Kaplan turbines. The dam is located in a trough-shaped valley with thick Quaternary fluvial sediments, mostly coarse sand and gravel pads. The bedrock consists of sedimentary rock formations of Upper Bakhtiari. River Valley lies on the regional tectonic line (Figure 3,4).

DESIGNED DAM PARAMETERS

- ► Type: Embankment earth-fill dam with central clay core
- ► Upstream side slope: 1:3.5
- ► Downstream side slope: 1:3.0
- ► Maximum height: 23 m
- ► Maximum base width: 148.0 m (in the toe of the dam)
- ► Crest width: 9.0 m
- ► Crest length: 1190 m
- ► Crest elevation: 300 m a.s.l.
- ► Dam body volume: 980,000 m3 (body); 128,000 m3 (clay core)
- ► Catchment area: 20,142 km2
- Reservoir area: 415 ha (at water level 296 m a.s.l.)

Reservoir volume: 31 mil. m3 (at water level 296 m a.s.l.)

DESIGNED HYDRO POWER STATION PARAMETERS

► Designed net head: 16.0 m

► Designed total discharge: 50 m3/s

► Type of units: 4 vertical Kaplan

► Max. Power output: 4x 8,000 Kw



Figure 2 Iraq's map

Figure 1 Part of Iraq's map showing the site of the dam

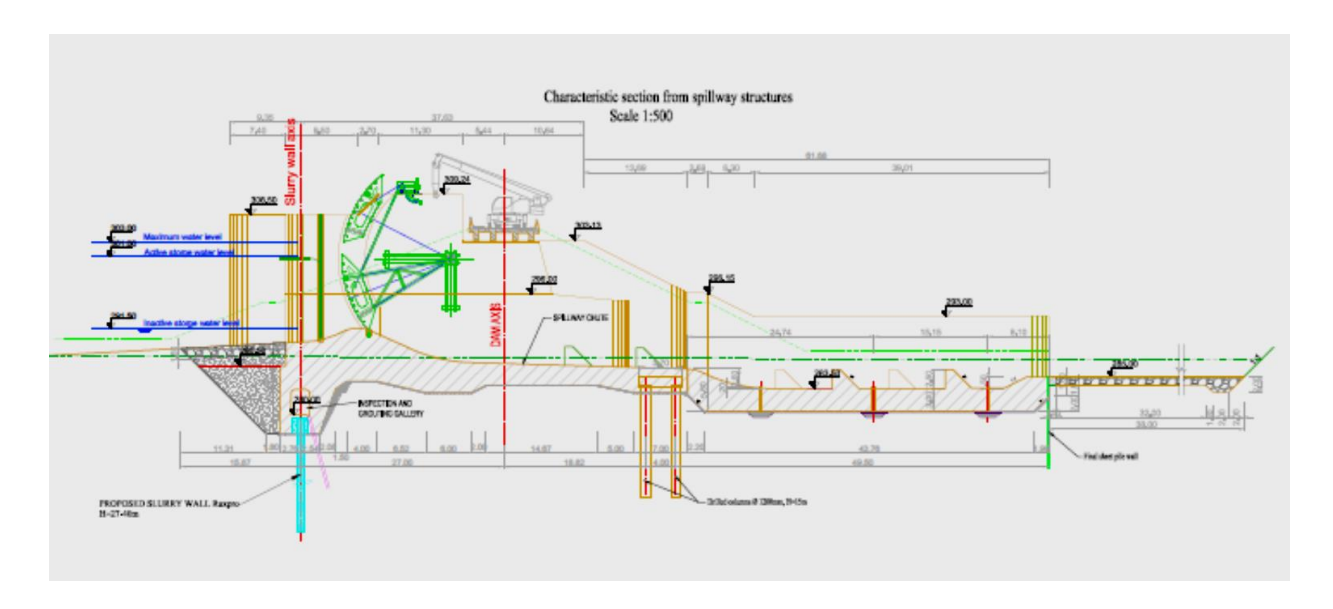


Figure 3 Spillway characteristic section

The spillway has only 6 bays equipped with 13,9 x 10,09 radial gates.

Reinforced concrete drill columns wall provided at the downstream toe of power house, spillway and bottom outlet structure.

An inspection and drainage gallery was provided along the upstream toe of all concrete structures.

A drainage system consisting of 15 m long, 300 mm diameter drill holes control the uplift underneath the concrete structures.

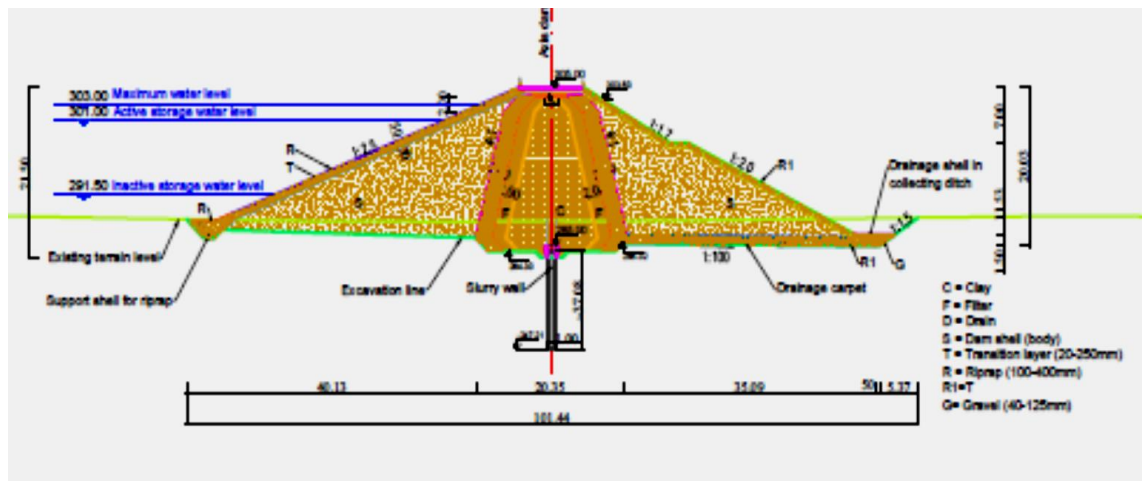


Figure 4 Earth dam characteristic section

The slopes of the dam are slightly steeper in accordance to the new seismic accelerations and the actual geotechnical characteristics of the available quarries.

Finite element method

Introduction

The Finite element method is a very powerful method for analytical calculation of different factors in concrete such as stress and thermal field in two or three dimensions, cracking parameters, interface problems, and others. Some of those effects and parameters are ignored or treated approximately in the past and this is why problems were not modeled rationally. However, experimental research did not stop with finite element development, it is still very important for comparison of finite element results with experimental results. Finite element method is based on a finite number of elements connected at a Finite number of joints (Campbell-Allen and Thorne 1963) .The modeling of the early age thermal behavior of conducted with the aid of the commercially available ANSYS software package. This software package was chosen because it offers a wide range of material models for the analysis of non-linear concrete material behavior including the behavior of young hardening concrete. It can make the assessment of the temperature development due to the cement hydration and the computation of the associated stress development within the concrete mass. The finite element analysis utilized ANSYS's 'staggered flow-stress analysis' feature, in which the thermal analysis is combined with a subsequent structural analysis. The model comprises two domains: one for the thermal flow analysis and one for the structural analysis, And so reside in a domain called the 'flow-stress domain'.

$$\rho C_p \frac{\delta_T}{\delta_t} = K(\frac{d^2T}{dx^2} + \frac{d^2T}{dy^2} + \frac{d^2T}{dz^2}) + Q_H$$
 (4)

where, C_p is the specific heat capacity, ρ is the density of the concrete, t is the time, k is the thermal conductivity, T is the temperature and Q_H , the rate of internal heat evolution, x, y, z are the coordinates at a particular point in the structure

This finite element model that was used to simulate the thermal behavior in mass concrete was verified or calibrated so that its temperature distribution for the entire volume closely match with that of the experimental block

ANSYS Finite Element Modeling

One of the goals of this project was to use a numerical modeling program to model mass concrete footings by predicting the spatial distributions of temperature throughout the concrete and its induced stresses. Using one such program, the temperature rise due to the internal early age hydration of the concrete and the correlating thermal gradients within the mass concrete can be computed. These thermal gradients then lead to induced thermal strains within the concrete due to internal and external restraints. Additionally, the evolution of the viscoelastic concrete mechanical properties, including elastic modulus, tensile strength, and shrinkage, can be modeled alongside the hydration induced temperatures as a function of time. The thermal strains combined with these concrete mechanical properties can then be translated into thermal stresses. When the resulting tensile thermal stresses are greater than the tensile strength of the concrete, cracking will occur.

ANSYS APDL was chosen due to its wide range of input possibilities and its 3D modeling capabilities, ANSYS's APDL ability to model the necessary thermal and mechanical properties. reinforcement and cooling mechanisms such as cooling pipes and thermal blankets made it an ideal program to use for the thermal analysis of early age mass concrete footings.

The commercial finite element software ANSYS APDL was ultimately chosen to analyze the Spillway of the BAWANUR DAM to its ability to model the temperature evolution of early age concrete during hydration as well as its nonlinear mechanical properties. This is accomplished through the program's wide range of thermal and mechanical input possibilities that tailor to the user's needs as well as through its 3D modeling capabilities.

THERMAL PROPERTIES

The flow of temperature throughout a 3D object is governed by two fundamental equations: the 3D extension of Fourier's law of conduction, as seen in Equation (5) assuming thermal conductivity is isotropic and homogeneous, and the increase of internal energy, as seen in Equation (6) (Mehta and Monteiro 2017). The law of energy conservation then states that the rate of heat transfer plus the rate of internal heat generation must equal the rate of increase of internal energy, which results in the Equation (7).

$$W = K(i\frac{\partial T}{\partial X} + j\frac{\partial T}{\partial y} + k\frac{\partial T}{\partial z})$$
(5)

$$S = \rho C_h \frac{\partial T}{\partial t} dx dy dz \tag{6}$$

$$K\left(i\frac{\partial^2 T}{\partial X^2} + j\frac{\partial^2 T}{\partial X^2} + k\frac{\partial^2 T}{\partial X^2}\right) + q = \rho C_h \frac{\partial T}{\partial t}$$
(7)

Where: w = the rate of heat transfer (J/hr)

s =increase of internal energy (J/hr)

q = rate of heat generation (J/hr)

k = thermal conductivity (J/m-hr-K)

 $\rho = \text{density } (\text{kg/}m^3)$

ch = specific heat (J/gram/K)

T(x,y,z) = the scalar temperature field

As one can see from Equation (7), the two important thermal properties that govern the heat flow within the concrete, aside from the internal heat generation caused by cement hydration, are its thermal conductivity and its specific heat. Thermal conductivity is the rate of heat flow through a unit area under a unit temperature gradient, or the ability of the material to conduct heat (R-07 2007). Specific heat on the other hand is the amount of heat required to Raise the temperature of a unity mass one degree. When specific heat is multiplied by the concrete density it becomes the thermal heat capacity per unit volume. These terms are related in Equation (8) through thermal diffusivity (h^2) . Diffusivity is the ability of the material to transmit heat or the ease at which a material can undergo temperature change, and is most significantly affected by

the thermal conductivity of aggregates in normal weight concretes.

$$Kh^2 = \frac{K}{\rho * C_h} \tag{8}$$

where: h^2) = diffusivity $(m^2)/hr$)

ANSYS APDL can model conductivity and heat capacity values as a function of time or temperature but was taken as constant for this research. A summary of the thermal properties input into ANSYS' APDL thermal model can be found in Table (2).

Material	Conductivity (J/m-hr°C)	Heat Capacity (J/m³-°C)
Concrete	7920	2675596
Plywood	540	85440
Steel	187200	3815100
Insulation Blankets	261	20824

Table 2 Material Thermal Properties

SOLID 70 Element Description

SOLID70 has a 3-D thermal conduction capability. The element has eight nodes with a single degree of freedom, temperature, at each node. The element is applicable to a 3-D, steady-state or transient thermal analysis. The element also can compensate for mass transport heat flow from a constant velocity field. If the model containing the conducting solid element is also to be analyzed structurally, the element should be replaced by an equivalent structural element (such as SOLID185). See SOLID90 for a similar thermal element, with mid-edge node capability Figure (5).

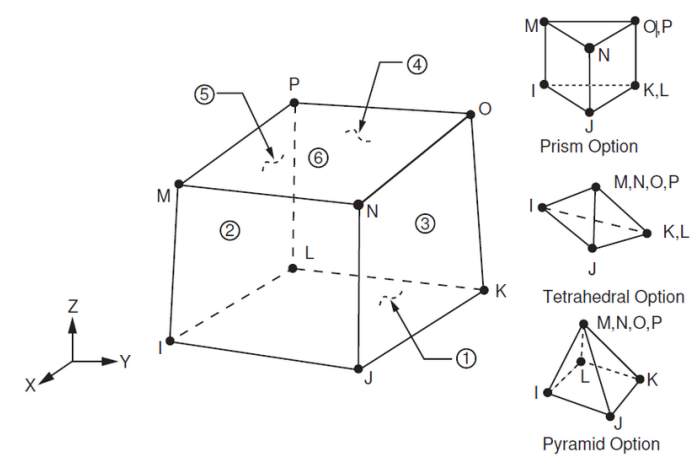


Figure 5 SOLID 70 Element

Boundary Conditions

The external environmental conditions were modeled by way of boundary elements on the outside surface of the model. The wind effects were first modeled through a forced convection term associated with the boundary elements to model the heat lost to the environment by an exposed surface Figure (7). ANSYS APDL uses Equation (9) to model the heat flow due to convection based on a convection

coefficient hc. This coefficient equation can be modeled as a function of time, a function of temperature, or remain constant.

$$qc = h As (Ts - TF) (9)$$

Where,

 q_c = the rate of heat transfer W/m²-°C

 T_s = temperature at the Surface °C

 T_F = Fluid temperature $^{\circ}$ C

 A_s = the surface area m²

h = the mean coefficient of heat transfer

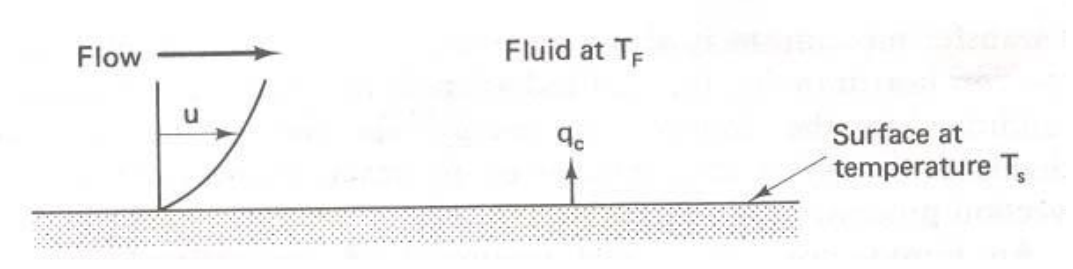


Figure 6(Convection heat transfer)

The heat lost and gained to the surrounding environment by the hydrating concrete's exposed surface and also the interaction of the foam with ambient conditions is modeled by imposing boundary convection elements. This is conveniently done using the convection element found in ANSYS to specify the convection and boundary conditions. The heat flow through the surface of the elements, q^S, due to convection is modeled by the following equation:

$$q^{S} = h_{c} \left(\theta_{e} - \theta^{S} \right) \tag{10}$$

Where:

 h_c = the convection coefficient, W/m²-°C

 θ_e = the external environment temperature, $^{\circ}C$

 θ^S = the surface temperature of the concrete block, °C

The convection coefficient can be constant, temperature-dependent, or time dependent. The convection coefficient was calculated using the equation

$$hc = \begin{cases} 5.6 + 3.95v, v \le 5\frac{m}{s} \\ 7.6v, v \ge 5m/s \end{cases}$$
 (11)

Where, v = the wind speed, m/s

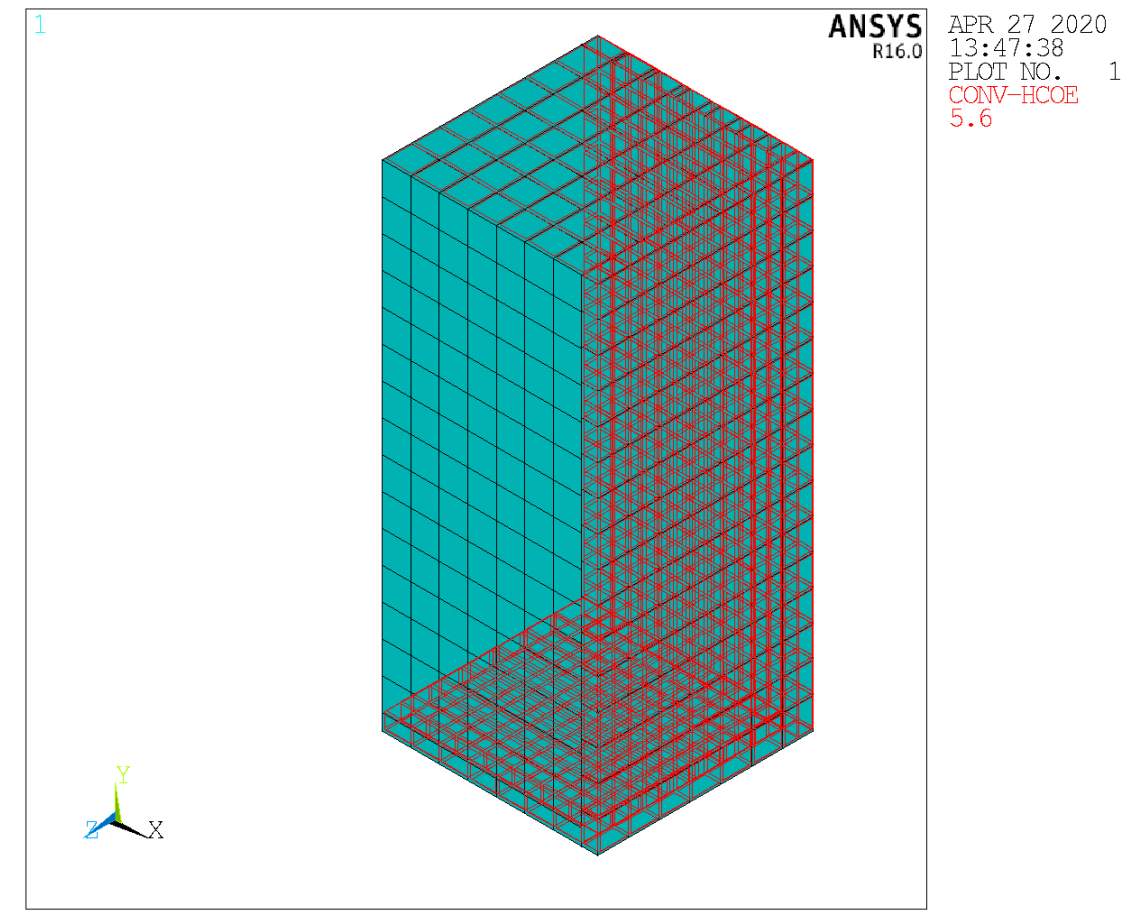


Figure 7 External temperatures imposed on finite element model representing the ambient conditions of the laboratory

ANSYS Finite Element spillway of BAWANUR DAM

Designed 2 Tainted gates of a span of 14.0 m and a height of 16 m (Designed net head: 16.0 m).

The work was divided at a height of 2 m for each stage (figures (8-16)) and the readings took six days 120 hours for each stage (figures (19-26)). The measurements were taken in the center of the body and near the surface and the readings were as:-

The thermal results from the analysis run in the center node, this location was chosen because it is where standards and specifications typically measure temperature and temperature differentials in these nodes.

- ► The model 2m above the base Rock predicted a maximum temperature of 66.2 °C to occur at 18 hours.
- ► The model 2m above the base concrete predicted a maximum temperature of 68 °C to occur at 17 hours.
- ► The model 4m above the base concrete predicted a maximum temperature of 68.3 °C to occur at 19 hours.
- ► The model 6m above the base concrete predicted a maximum temperature of 69.1°C to occur at 20 hours.
- ► The model 8m above the base concrete predicted a maximum temperature of 67.9 °C to occur at 20 hours.
- ► The model 10m above the base concrete predicted a maximum temperature of 68.4 °C to occur at 18 hours.
- ► The model 12m above the base concrete predicted a maximum temperature of 67.0286 °C to occur at 18 hours.
- ► The model 14m above the base concrete predicted a maximum temperature of 67.9°C to occur at 20 hours.
- ► The model 16m above the base concrete predicted a maximum temperature of 69.1°C to occur at 20 hours.

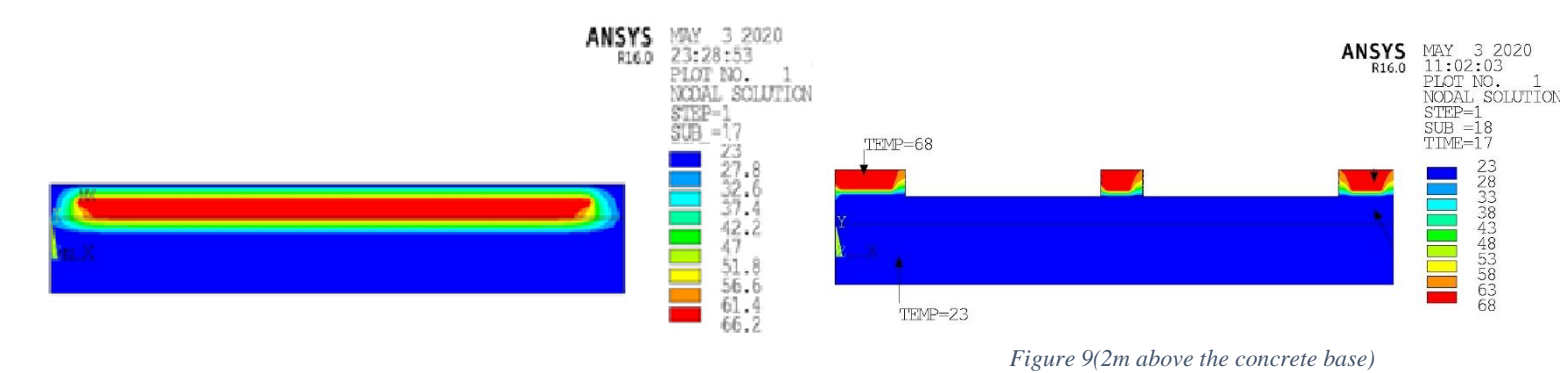


Figure 8(2m above the Rocks)

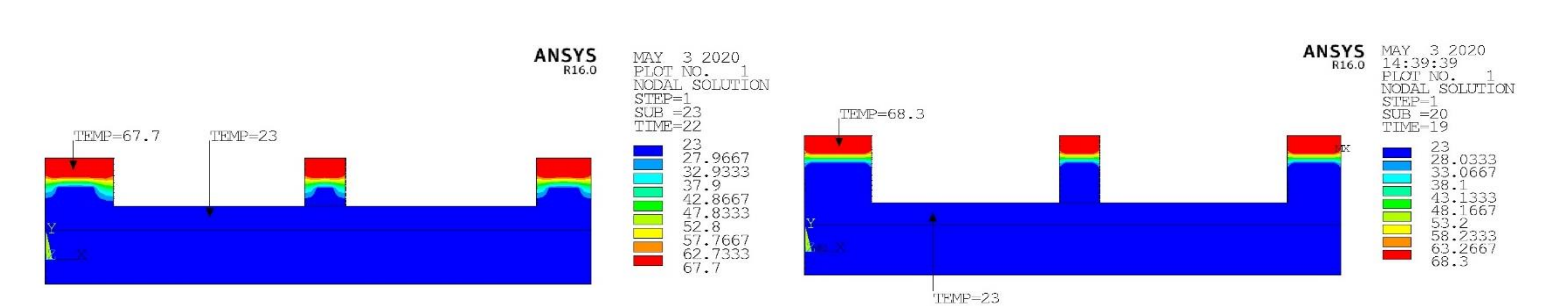


Figure 11(4m above the concrete base)

Figure 10(6m above the concrete base)

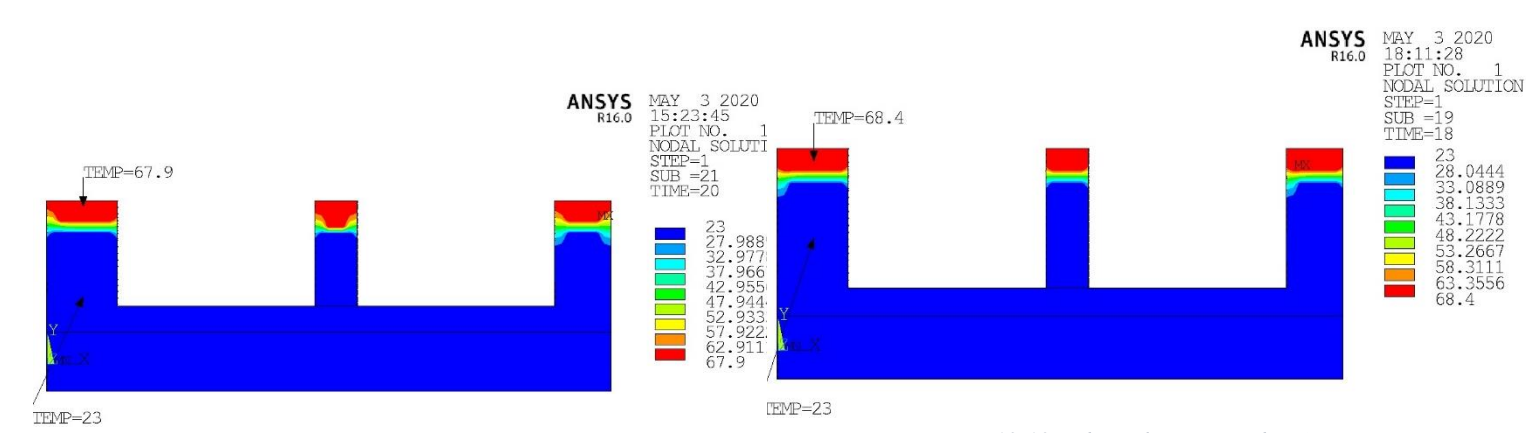


Figure 12(8m above the concrete base)

Figure 13(10m above the concrete base)

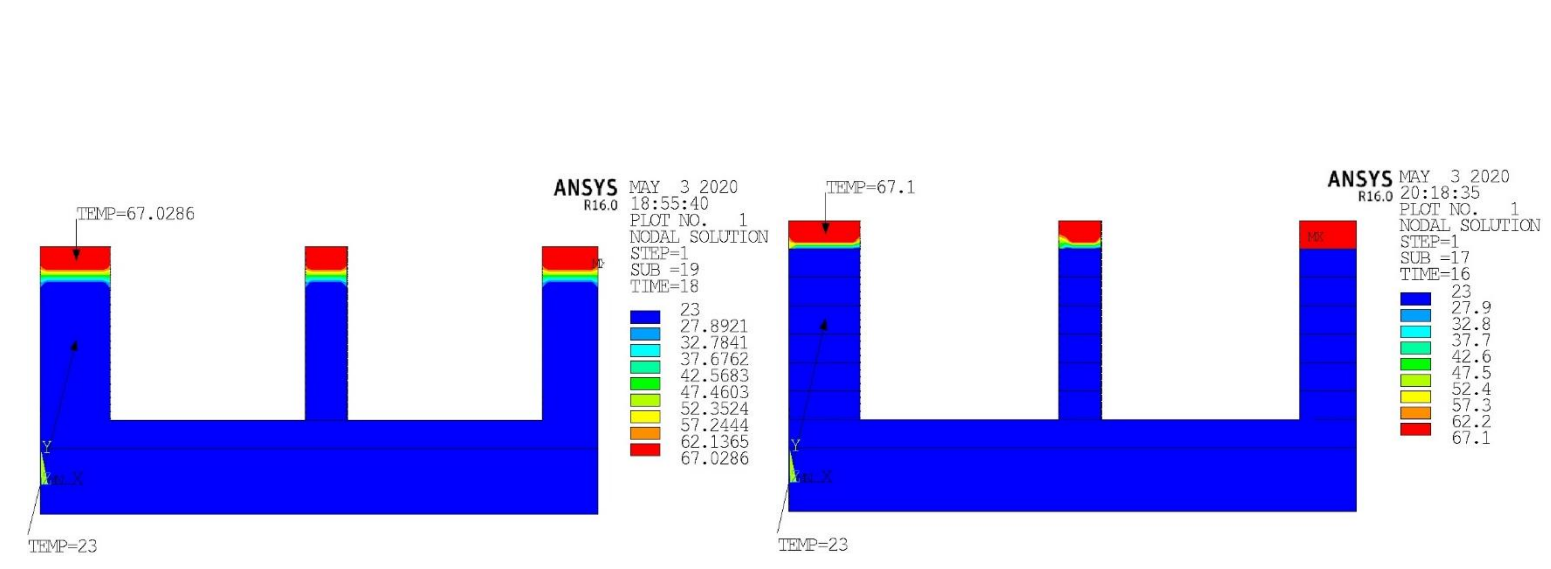


Figure 15(12m above the concrete base)

Figure 14(14m above the concrete base)

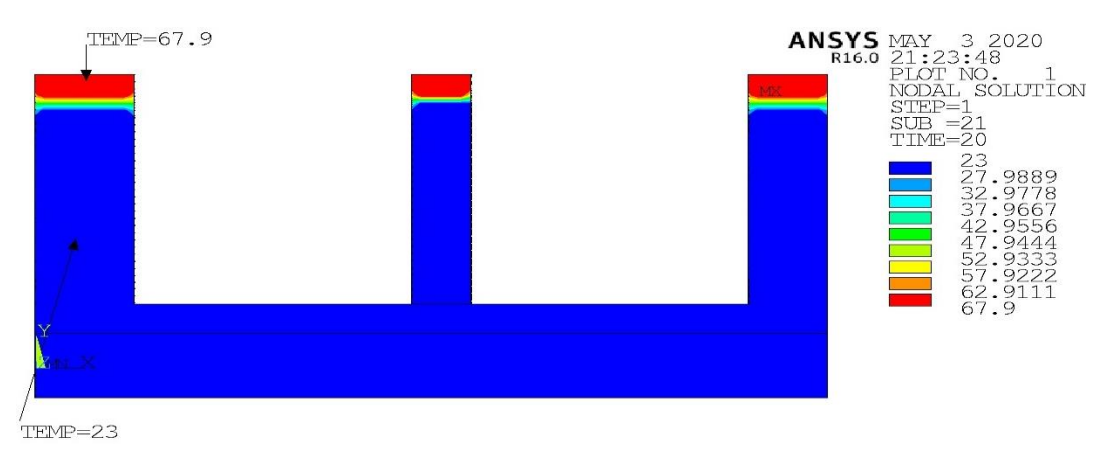


Figure 16(16m above the concrete base)

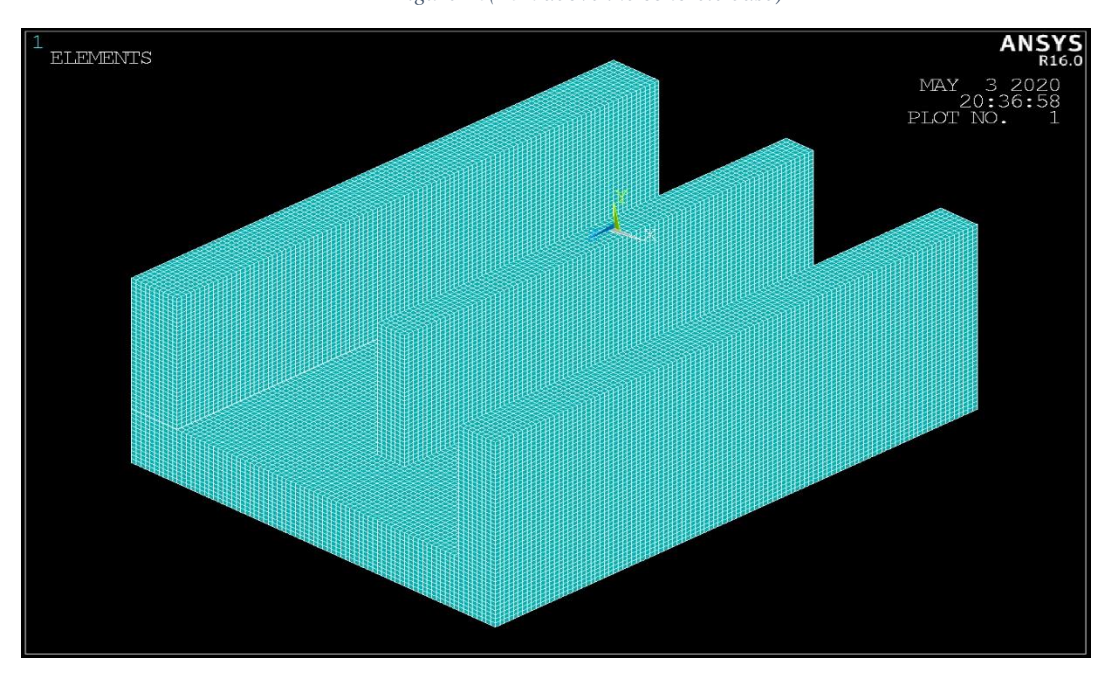


Figure 17 (meash 16m above concrete base)

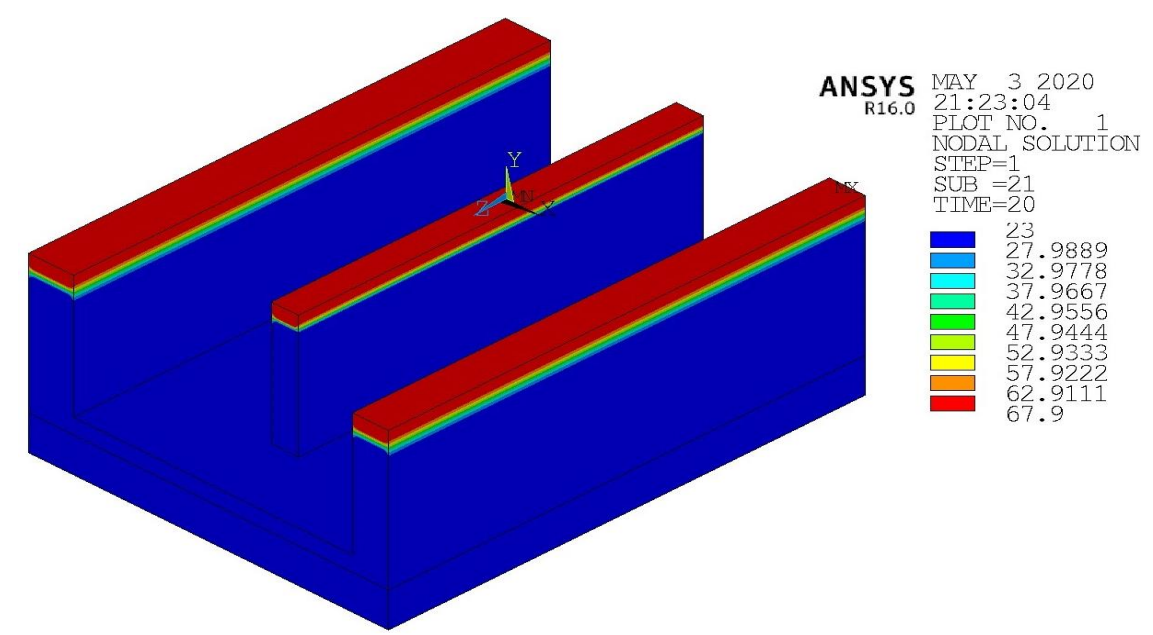


Figure 18(16 m above concrete base tot.)

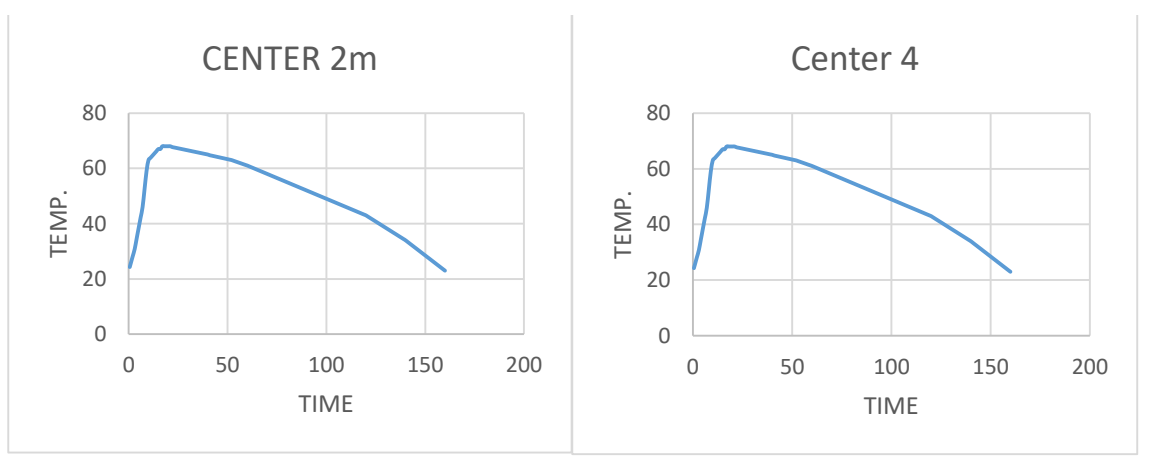


Figure 19(2m above the concrete base the NODE CENTER) Figure 20(4m above the concrete base the NODE CENTER)

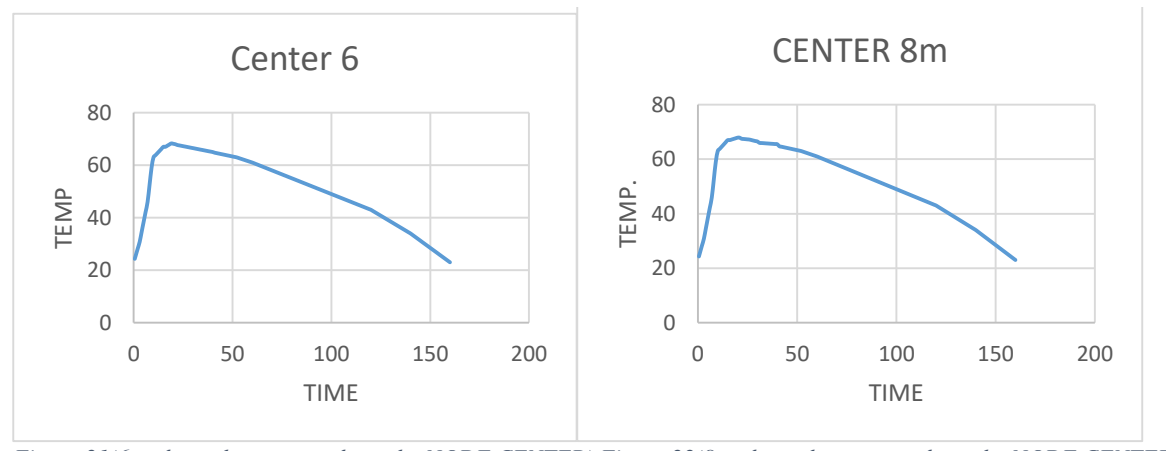


Figure 21(6m above the concrete base the NODE CENTER) Figure 22(8m above the concrete base the NODE CENTER)

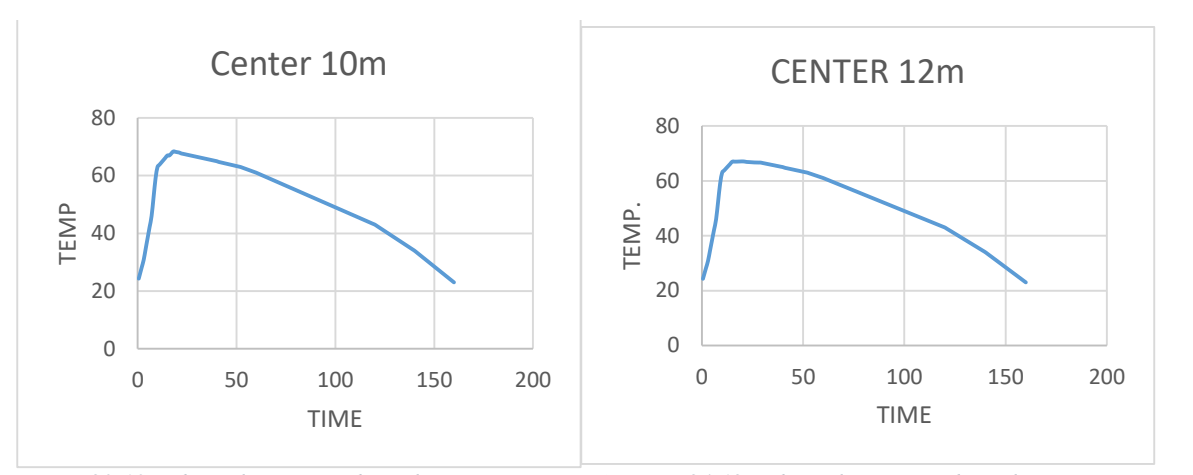


Figure 23(10m above the concrete base the NODE CENTER) Figure 24(12m above the concrete base the NODE CENTER)

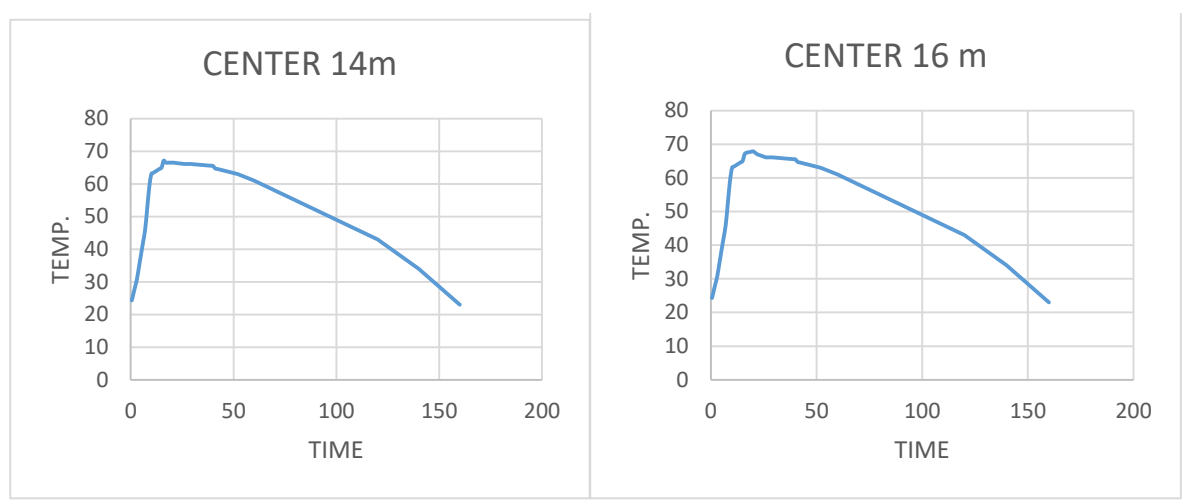


Figure 25(14m above the concrete base the NODE CENTER) Figure 26(16m above the concrete base the NODE CENTER)

MASS CONCRETE BLOCK EXPERIMENT (Lawrence 2009)

Introduction

This chapter deals with the results produced by the finite element numerical model. Comparisons between the predicted and measured results obtained from the experiment are then drawn. The profiles that were utilized for a comparison verification exercise are:

The experiment was the mass concrete block experiment was set up in UNIVERSITY OF FLORIDA in the United States. (Lawrence 2009).

To verify that the finite element model created is effective in modeling the earlyage behavior of hydrating mass concrete, four different mixes of concrete, typical of use in mass concrete applications in Florida, were produced. Each mixture was used to make large concrete blocks with dimensions that qualify them to be characterized as massive concrete elements. Measurements of the temperature and strain at predetermined locations within the blocks were recorded until the equilibrium temperature was achieved. These temperatures and strains will then be compared with the results obtained from the finite element model. The results of the first mixture were compared in this report.

Furthermore, this chapter presents a detailed comparison between the predicted three-dimensional temperature profiles using finite element and finite difference analysis techniques. Comments and proposed solutions to errors within the modeling techniques are also discussed. This section will commence with an explanation of the input variables required to obtain a solution from the finite element numerical model - accurate input variables are the fundamental basis for the prediction of valid solutions. The results of the finite element numerical model, including a comparison with the measured and finite-difference model results, are then presented. A sensitivity analysis, demonstrating the effect of various element configurations on the predicted results, will bring the model output portion to a close.

Block Geometry

Two 42" x 42" (1.07m x 1.07m x 1.07m) forms were created for the pouring of the experimental concrete blocks. The geometry of the blocks is presented in Figure 26. The side faces and base of both blocks consisted of a 0.75-inch thick plywood formwork surrounded by a 63 three inches thick layer of polystyrene plates. However, one of the blocks had a cover with the same makeup as the sides placed on its top surface after the pouring was completed in an effort to simulate a fully adiabatic process, while the top face of the other block was left open and exposed to environmental conditions. Figure (27) is a photograph of the two blocks after the concrete had been poured.



Figure 27 Uninsulated (left) and insulated (right) mass concrete block specimens

Instrumentation for Data Collection Introduction

The two concrete blocks were instrumented for the monitoring of early age temperatures and strain at predetermined locations. The data acquisition equipment consisted of Type K thermocouples with an accuracy of ± 2.2 °C and embedded strain gages Figure 28.

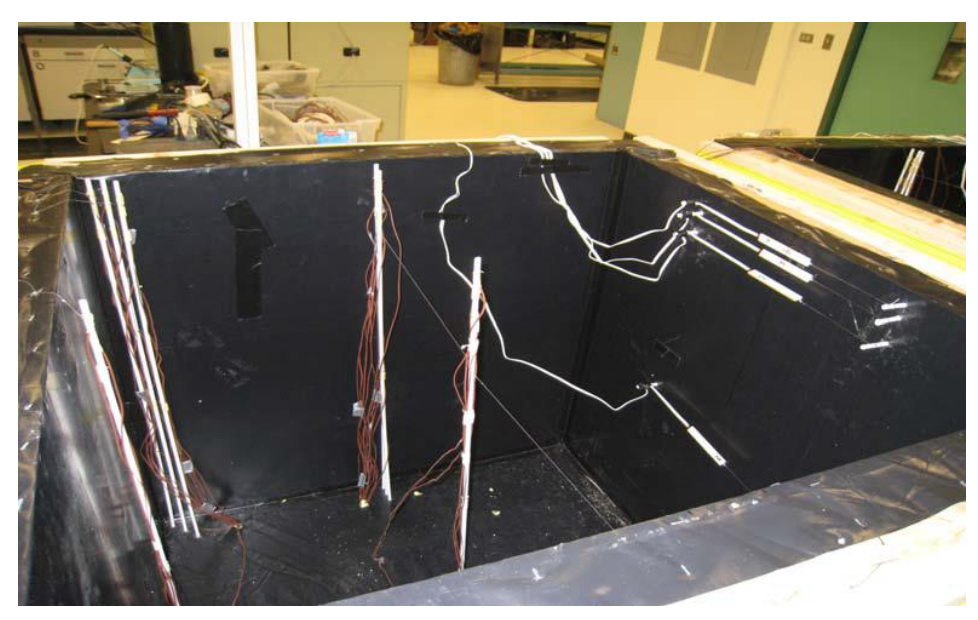


Figure 28 Steel reinforcement cage with thermocouples attached. (The red circles highlight locations of the exposed thermocouples.)

Temperature Profiles

The location of the thermocouples in the blocks were chosen to capture the temperature difference between the center of the block and the exposed surface, as well as to monitor the near surface temperature gradient to determine if it would contribute to thermal cracking of the concrete. The thermocouples at the sides and bottom of the block were placed to validate the effectiveness of the insulation and by extension the thermal boundary conditions that would be used in the finite element model Table 3.

MASS CONCRETE MIX DESIGN				
	Mix 1	Mix 2	Mix 3	Mix 4
	100% Portland	50% Portland	65% Portland -	50% Portland
	cement (Ib/yd3)	50% Slag	35% Fly	30% Slag -
		(Ib/yd3)	Ash(Ib/yd3))	20% Fly
				Ash(Ib/yd3))
Cement	681	341	443	341
Fly Ash	0	0	238	136
GGBF Slag	0	341	0	204
water	341	341	341	341
Fine Agg.	1095	1088	1036	1050
COURSE Agg.	1668	1668	1660	1650

Table 3 Thermal properties of concrete

	CONDUCTIVI	HEAT	ACTIVATION
	TY	CAPACITY	ENERGY
	$(J/m-hr-^{\circ}C)$	$(J/m^3-{}^{\circ}C)$	(J/mol)
Mixture 1	7920	2675596	34235
Mixture			
2	4418	2017434	50400
Mixture			
3	5883	2603101	32982
Mixture			
4	4838	2024985	37330

Table 4 Mechanical properties of concrete

Model Geometry

Figure 29 shows the model with dimensions (2.5, 1.5, and 2.5) m, depicting the concrete exposed to ambient conditions at the top surface and with the plywood and polystyrene insulation at the bottom and sides. To improve the efficiency of the analysis, the advantage was taken of the double symmetry of the block which allowed for the modeling of one-quarter of the block.

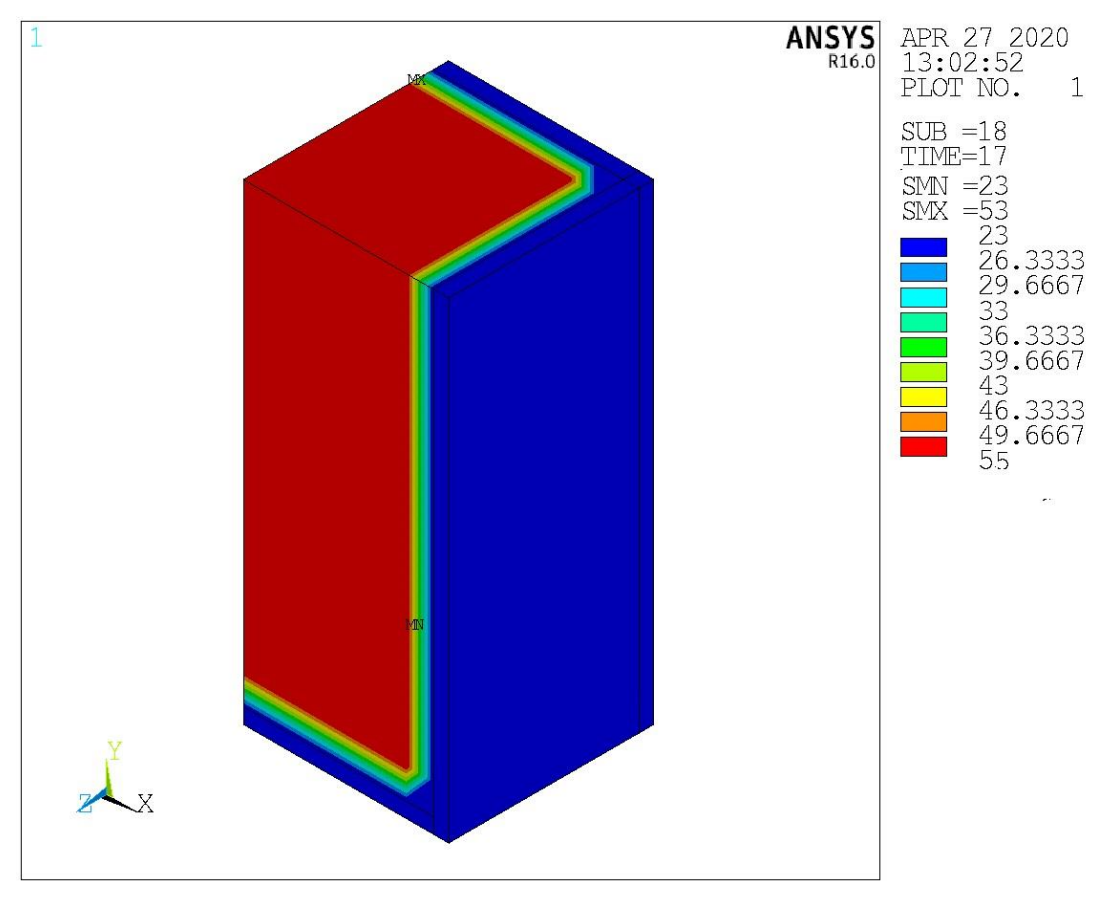


Figure 29 Finite element model of concrete block with insulation at time 17 hr.

Chapter 4: FINITE ELEMENT ANALYSIS RESULTS

Thermal Analysis Results

The thermal results from the analysis run were compared to the measured results from the experiment. Points 2 inches, 4 inches, and 21 inches below the top surface along the centerline of the block were chosen for the analysis in Figure 28. These locations were chosen because it is where standards and specifications typically measure temperature and temperature differentials.

The block temperatures 21 inches below the top surface of the block are presented in Figure 31. The experimental temperatures are represented by blue lines and the predicted temperatures from the model are represented by red lines. As these figures indicate, the finite element model was able to accurately capture and model the temperature distribution measured in the concrete block.

The model predicted a maximum temperature of 69.1°C to occur at 19 hours and start decreasing at 28 hours, whereas the actual measured maximum temperature was found to be 67.2°C at 20 hours after the pour and was found to decrease after 28 hours.

The block temperatures 4 inches below the top surface of the block are presented in Figure 32. The model predicted a maximum temperature of 55 °C to occur at 17 hours and start decreasing at 27 hours, whereas the actual measured maximum temperature was found to be 53.34 °C at 21 hours after the pour and was found to decrease after 25 hours.

The finite element model was able to fairly accurately predict temperature differentials measured in the concrete block due to its accurate prediction of the temperature distribution.

the maximum difference between the top surface and the center is 17.95° C to occur at 41 hours this amount is below temperature differentials (35°C) allowable Figure 33.

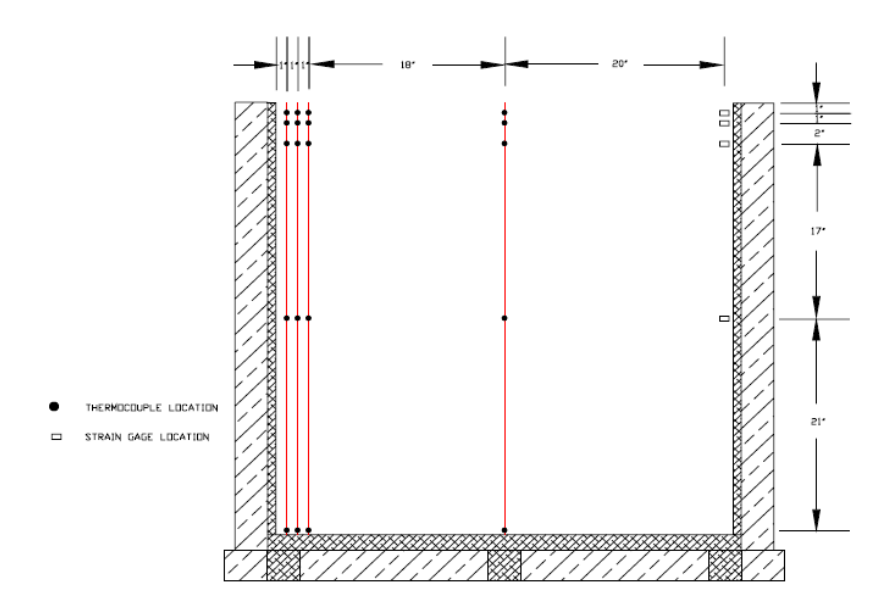
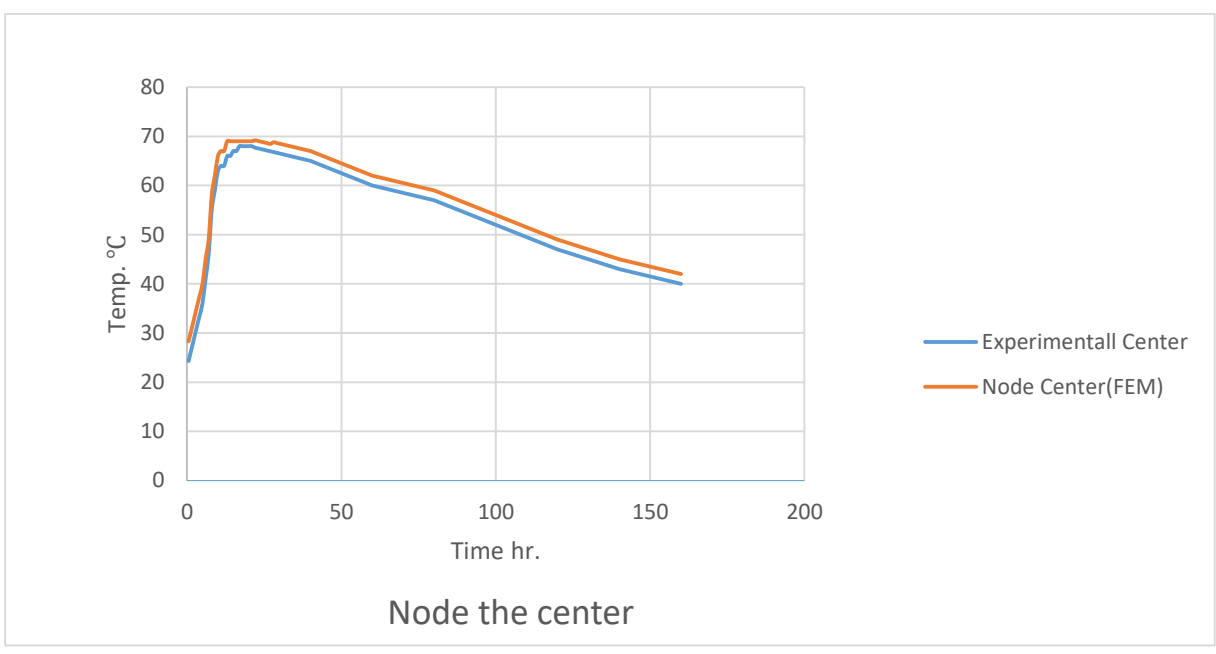
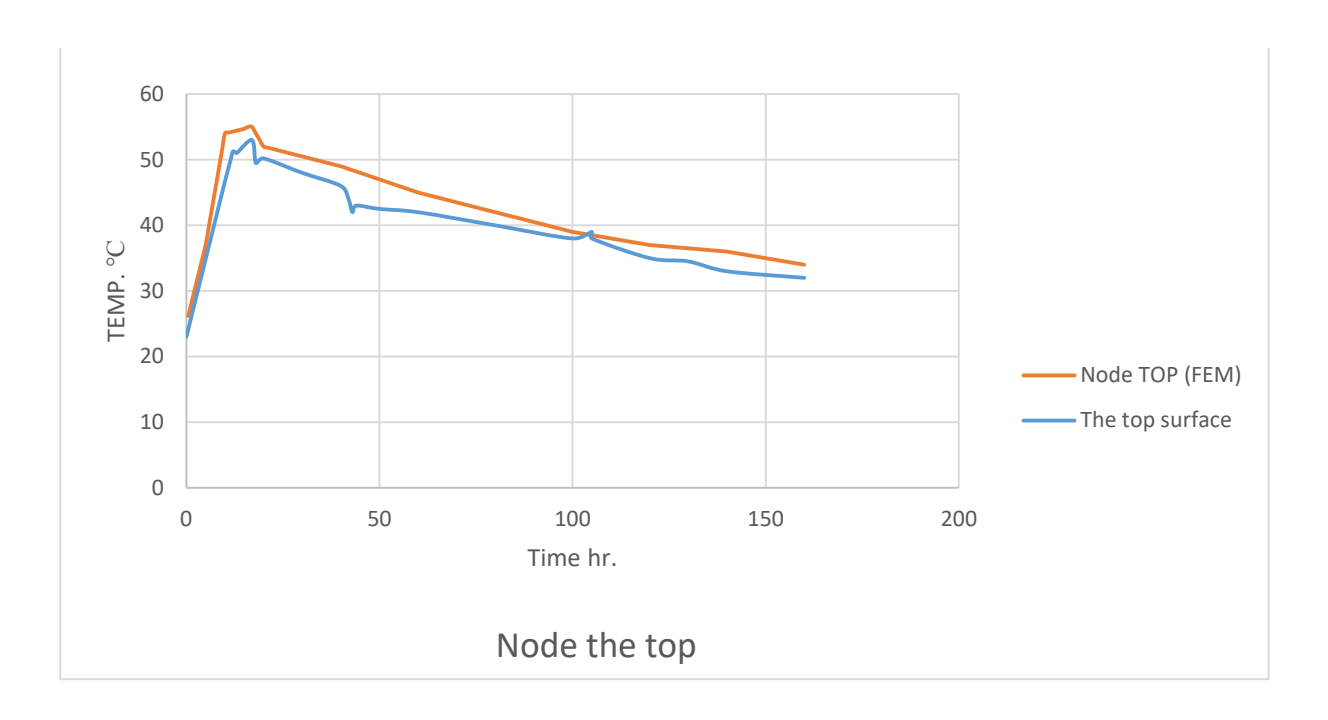


Figure 30 Thermocouple location (Section)



Figure~31~Semi-adiabatic~and~experimentally~measured~temperature-time~histories~at~the~center~of~the~block,~21"~below~the~exposed~top~surface~of~mixture~1



Figure~32~Semi-adiabatic~and~experimentally~measured~temperature-time~histories~at~the~center~of~the~block,~2"~below~the~exposed~top~surface~of~mixture~1

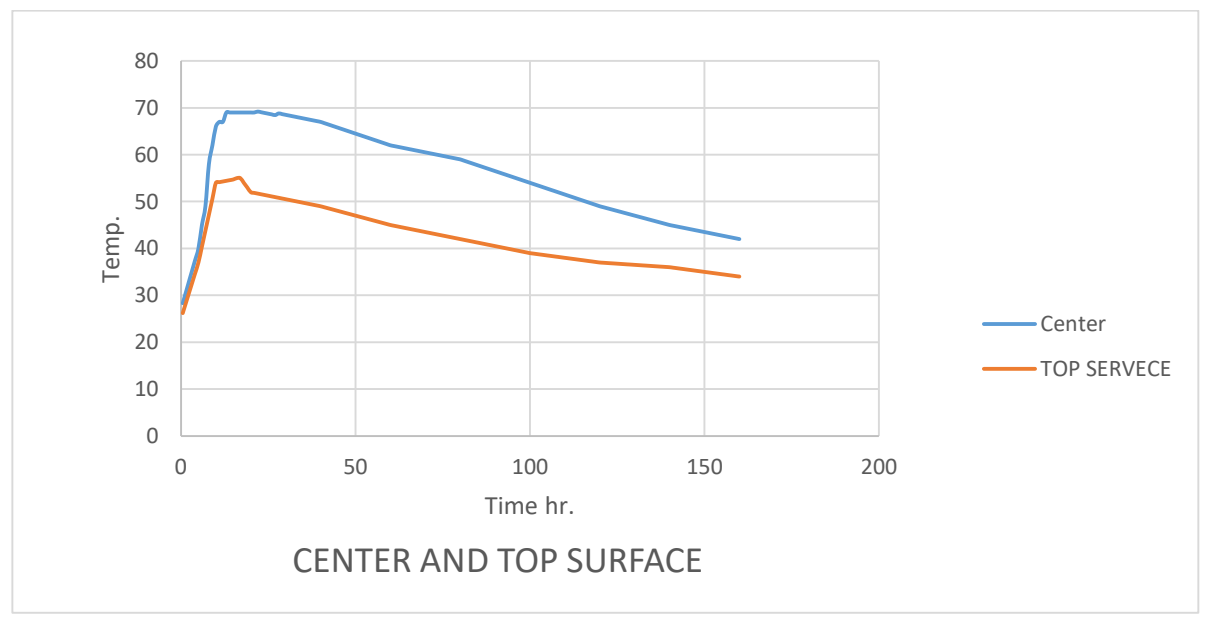


Figure 33 Comparison of the center and the upper surface

Structure Analysis Results

Overview of Finite Element Structural Model

The temperature distribution obtained from the thermal analysis was applied by (Switch Element type thermal to the structure). Crack formation and growth cause failure of concrete structures. Stress evaluation is one of the major tasks in concrete structures. Due to the heat of hydration of cement in early age mass concrete, stresses are not negligible. Mathematically, these stresses will disappear after some time, but this is not the case in reality. Before the structure enters in service, it is already pre-stressed. Stresses stay captured in the structure and are self-equilibrating. We must know the maximum stress as residual stress in a structure that occurs as a result of thermal load.

The heat produced during the hydration of concrete causes an increase in its temperature. However, because of the inhomogeneous hydration within the concrete element and the inhomogeneous loss of heat to the surrounding environment, temperature differences will occur throughout the concrete element. These temperature differences can induce thermal strains and stresses that could potentially initiate cracking if they exceed the early age tensile strength of the concrete. The temperature distribution solution obtained from the thermal analysis is imposed as a thermal load in the structural analysis of the concrete. The mechanical response to the stresses induced by the thermal gradient is greatly dependent on the physical characteristics of the concrete.

Material Model

To model the elasticity of the concrete, the Young's modulus E, Poisson's ratio v, and coefficient of thermal expansion α , were directly input into the model.

The potential for cracking is tracked by specifying the tensile strength evolution by way of a discrete function that is dependent on time.

Modulus of Elasticity

Cracking in mass concrete occurs when the tensile stresses induced by the thermal gradients are greater than the tensile strength. The modulus of elasticity (MOE) of concrete is the ratio between the stress and reversible strain and is important because it influences the rigidity of the concrete structure. This linear relationship is known as Hooke's Law and is expressed in Equation 12,

$$\sigma = E \varepsilon \tag{12}$$

Where σ = stress (MPa) E = Young's Modulus (MPa), ε = linear strain.

The elastic limit represents the maximum allowable stress before the concrete will crack and undergo permanent deformation. In heterogeneous multiphase materials like concrete, the modulus of elasticity increases as it hydrates, which is detrimental to the concrete because the probability of cracking increases as the modulus increases. To correctly model the thermal stresses in young concrete, it is essential to include the variation of the mechanical properties with time of the concrete (De Schutter and Structures 2002), most importantly the elastic modulus. Therefore, testing for the tensile modulus of elasticity of concrete at early ages is needed for input parameters of modeling.

Poisson's Ratio

Poisson's ratio is the ratio of the lateral strain to the axial strain within the elastic range of the concrete. According to (Mehta and Monteiro 2017), Poisson's ratio has no consistent relationship with the curing age of the concrete. Values obtained during the testing for compression modulus of elasticity were consistently 0.2, which is within the universally accepted range of 0.15 and 0.20 for concrete.

Coefficient of Thermal Expansion

The coefficient of thermal expansion is used to describe the sensitivity of concrete expansion or contraction to changes in temperature. It is defined as the change in unit length per degree of temperature change(Mehta and Monteiro 2017). The value of the coefficient of thermal expansion is particularly important in mass concrete because the strain induced during the cooling period is dependent on both the magnitude of the change in temperature and the coefficient of thermal expansion

Stress Results

Figure 34 presents the calculated stress in the model, a spillway of the BAWANUR DAM, with 16m concrete above the base concrete. Calculated by the finite element method by ANSYS APDL program in the X-X plane (max stress 1.42695 and the min stress occur -2.26127), occurring at a time at 20 hours where the maximum temperature occurs.

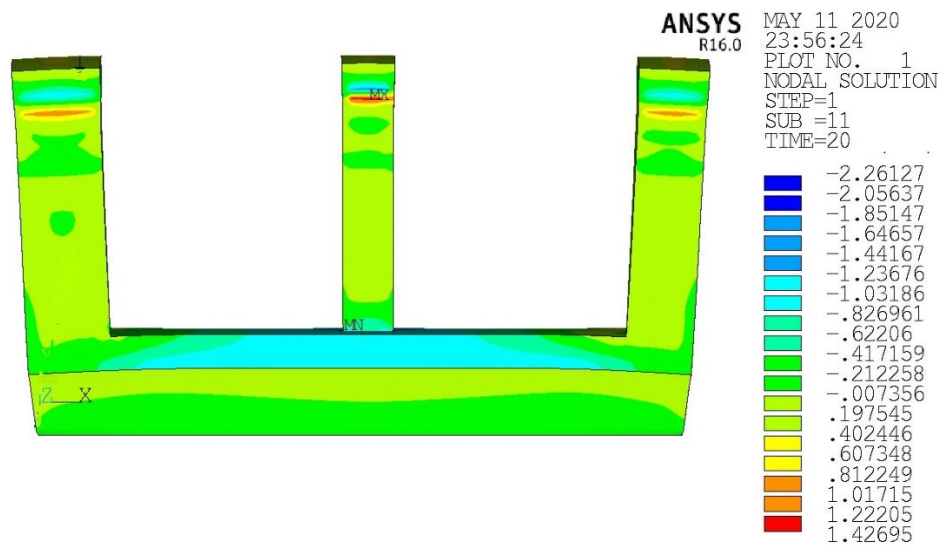


Figure 34(Principle stress in the x-x plane with the 16m above the concrete base)

Figure 35 presents the calculated Von Mises stress in the model, a spillway of the BAWANUR DAM, with 16m concrete above the base concrete. Calculated by the finite element method by ANSYS APDL program (max stress 5.92715 and the min stress occur 0.018355), occurring at a time at 20 hours where the maximum temperature occurs.

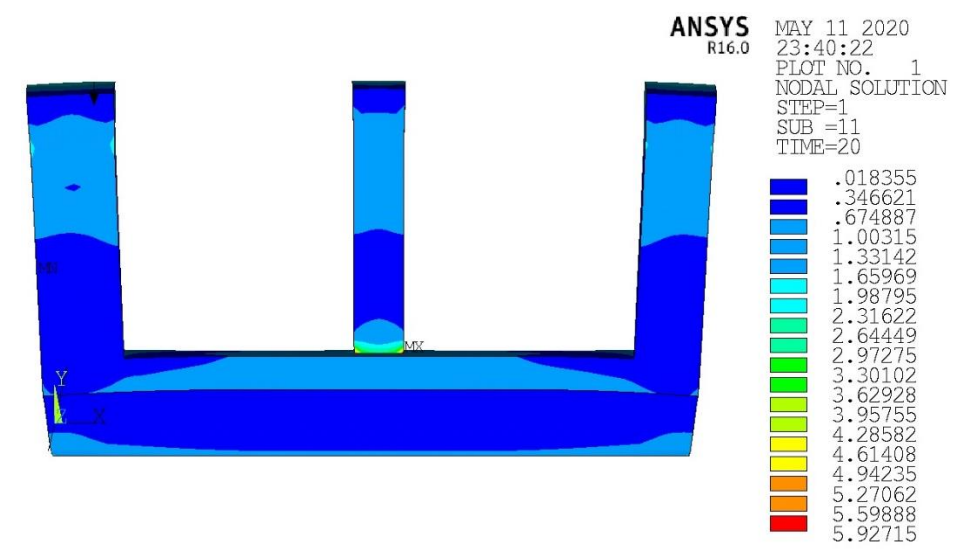


Figure 35(Von Mises stress with the 16m above the concrete base)

Figure 36 (3-D) presents the calculated stress in the model, a spillway of the BAWANUR DAM, with 4 m concrete above the base concrete. Calculated by the finite element method by ANSYS APDL program in the X-X plane (max stress 0.827249 and the min stress occur -2.02887), occurring at a time at 19 hours where the maximum temperature occurs.

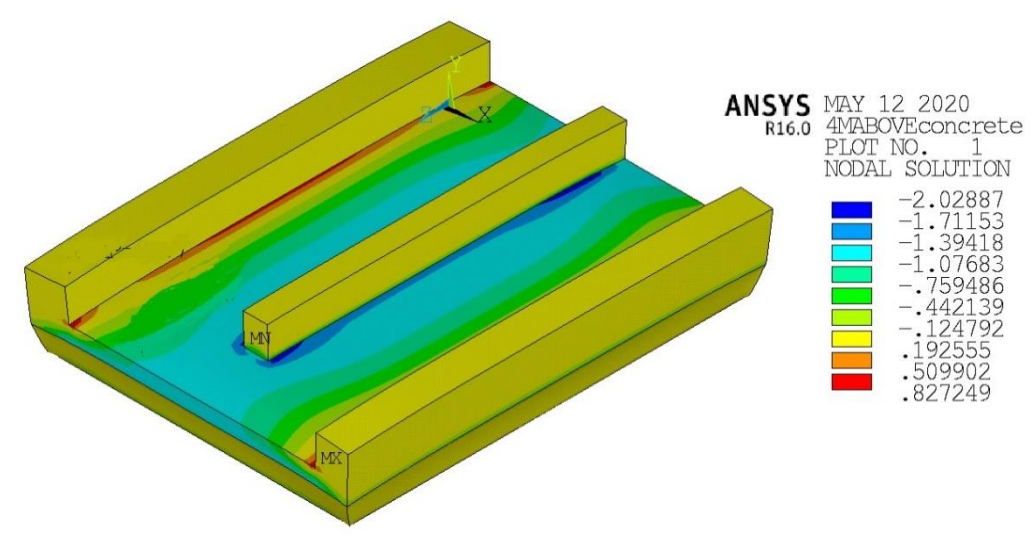


Figure 36 (Principle stress in the x-x plane with the 4m above the concrete base 3D)

Figure 37 (C-S) presents the calculated stress in the model, a spillway of the BAWANUR DAM, with 4 m concrete above the base concrete. Calculated by the finite element method by ANSYS APDL program in the X-X plane (max stress 0.827249 and the min stress occur -2.02887), occurring at a time at 19 hours where the maximum temperature occurs.

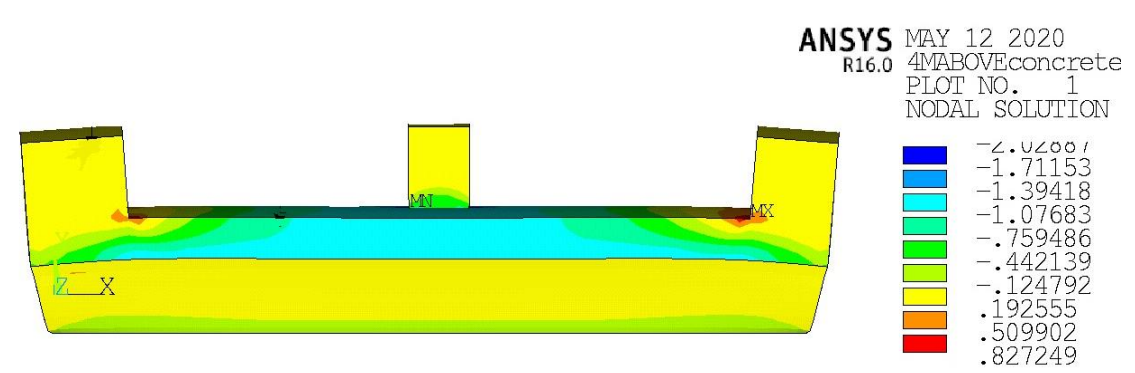


Figure 37(Principle stress in the x-x plane with the 4m above the concrete base cross section)

Figure 38 (3-D) presents the calculated Von Mises stress in the model, a spillway of the BAWANUR DAM, with 4 m concrete above the base concrete. Calculated by the finite element method by ANSYS APDL program (max stress 3.45127 and the min stress occur 0.07603), occurring at a time at 19 hours where the maximum temperature occurs.

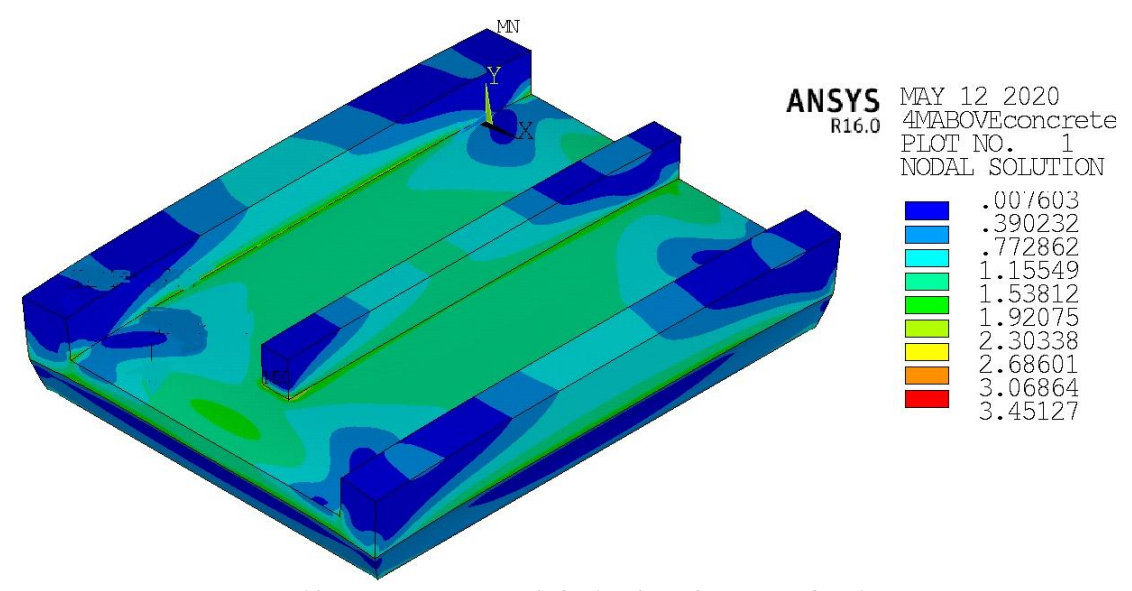


Figure 38(Von Mises stress with the 4m above the concrete base3D)

Figure 39 (C-S) presents the calculated Von Mises stress in the model, a spillway of the BAWANUR DAM, with 4 m concrete above the base concrete. Calculated by the finite element method by ANSYS APDL program (max stress 3.45127 and the min stress occur 0.07603), occurring at a time at 19 hours where the maximum temperature occurs.

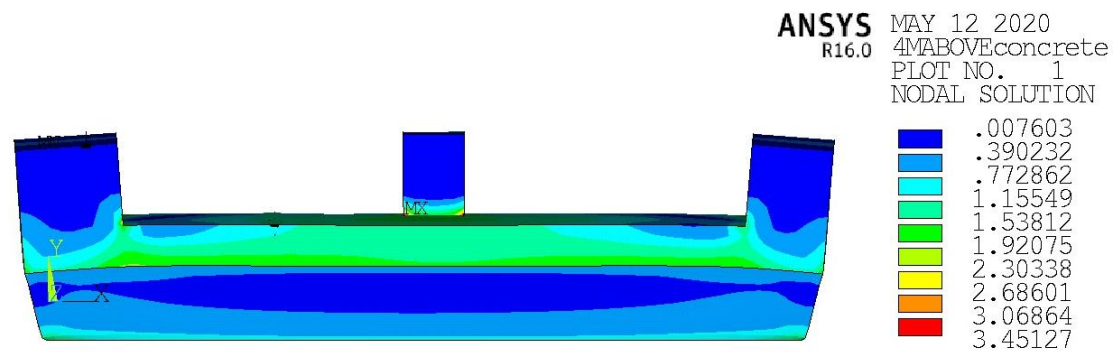


Figure 39(Von Mises stress with the 4m above the concrete base c.s)

Figure 40 presents the calculated principal stress from the finite element method by ANSYS APDL program in the X-X plane 3-Dimension compare with the experimental (max stress 2.94497 and the min stress occur 0.056698), occurring in the block with time at 20 hours where the maximum temperature occurs.

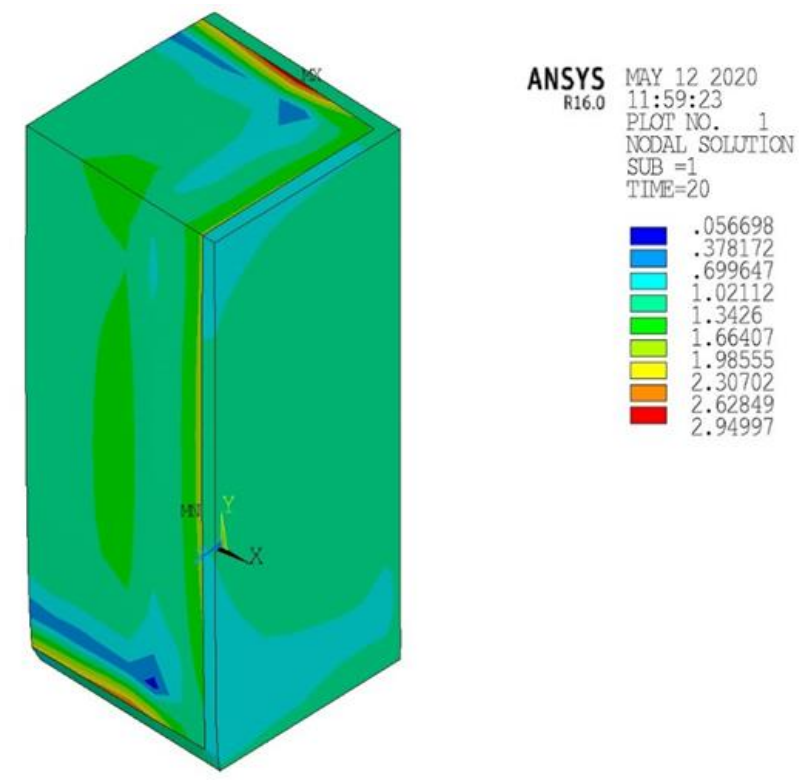


Figure 40(Principle stress in the x-x plane)

Figure 41 presents the calculated Von Misess stress from the finite element method by ANSYS APDL program, 3-Dimension compare with the experimental (max stress 5.09183, and the min stress occur -3.00031), occurring in the block with time at 20 hours where the maximum temperature occurs.

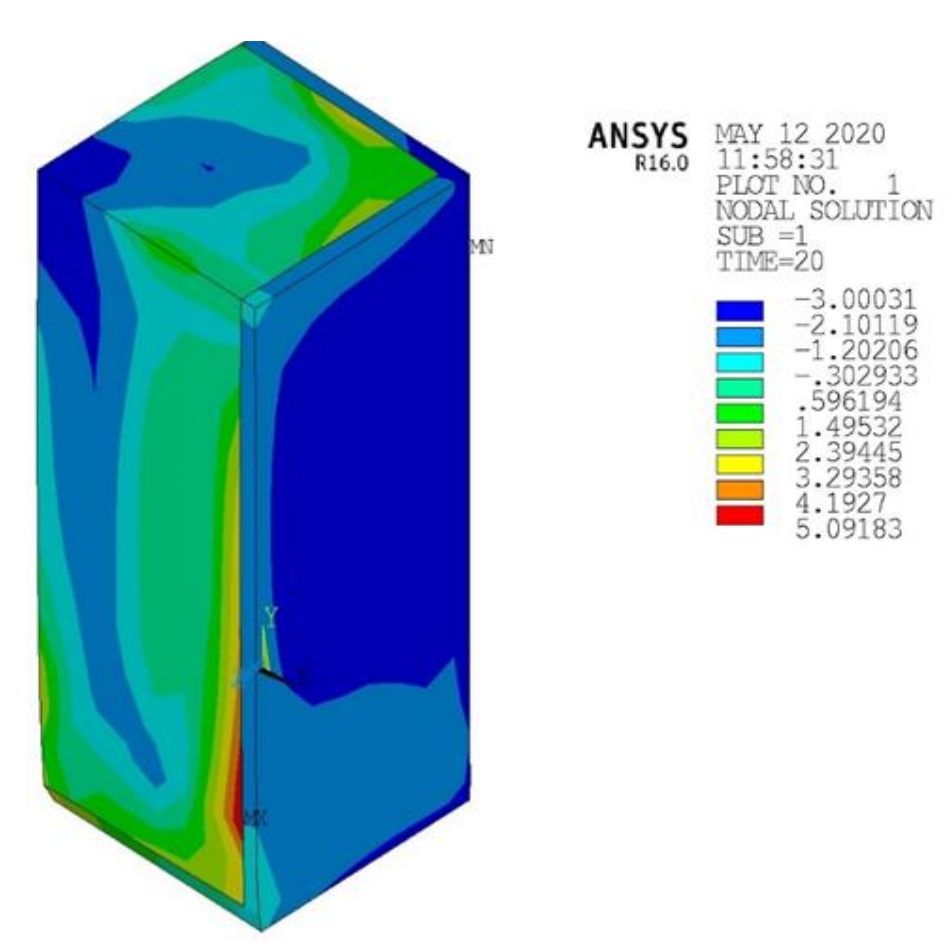


Figure 41(von Mises stress)

Conclusion

The temperatures were predicted very accurately and calculated the stress by doing the switch thermal to structure in ANSYS PROGRAM. the spillway of the BAWANUR DAM IN IRAQ at various stages and the results were very close to the literature in this specialty and the results are as follows:-

- The model 2m above the base Rock predicted a maximum temperature of 66.2 °C to occur at 18 hours. The model 2m above the base concrete predicted a maximum temperature of 68 °C to occur at 17 hours. The model 4m above the base concrete predicted a maximum temperature of 68.3 °C to occur at 19 hours. The model 6m above the base concrete predicted a maximum temperature of 69.1 °C to occur at 19 hours. The model 8m above the base concrete predicted a maximum temperature of 67.9 °C to occur at 20 hours. The model 10m above the base concrete predicted a maximum temperature of 68.4 °C to occur at 18 hours. The model 12m above the base concrete predicted a maximum temperature of 67.0286 °C to occur at 18 hours. The model 14m above the base concrete predicted a maximum temperature of 67.9 °C to occur at 20 hours. The model 16m above the base concrete predicted a maximum temperature of 69.1 °C to occur at 20 hours.
- The calculated stress in the model, with 16m concrete above the base concrete. In the X-X plane (max stress 1.42695 and the min stress occur 2.26127), occurring at a time at 20 hours where the maximum temperature occurs.
- The calculated Von Mises stress in the model, (max stress 5.92715 and the min stress occur 0.018355), occurring at a time at 20 hours where the maximum temperature occurs.
- The calculated stress in the model in the X-X plane (max stress 0.827249 and the min stress occur -2.02887), occurring at a time at 19 hours where the maximum temperature occurs.
- The calculated Von Mises stress in the model, (max stress 3.45127 and the min stress occur 0.07603), occurring at a time at 19 hours where the maximum temperature occurs.

- A finite element model was developed using the ANSYS APDL commercial software to model the heat generation and temperature distribution created during concrete early age hydration. The predicted temperatures from the block experiment to actual measured temperatures to validate the accuracy of the developed model. Analysis of the results from these models and their comparisons to the measured data resulted in the following findings:
 - The finite element model created in ANSYS APDL accurately predicts the heat production and subsequent temperature changes during early age concrete hydration.
 - The biggest temperature differentials were found to occur between the center and the top surface is 17.95 below temperature differentials (35 °C) allowable.
- The model predicted a maximum temperature of 69.1°C to occur at 20 hours in the center nodes.
- The model predicted a maximum temperature of 55 °C to occur at 17 hours in the near top surface.
- The calculated principal stress (max stress 2.94497and the min stress occur 0.056698), occurring in the block with time at 20 hours where the maximum temperature occurs.
- The calculated Von Misess stress (max stress 5.09183, and the min stress occur -3.00031), occurring in the block with time at 20 hours where the maximum temperature occurs.
- Reliance on a limiting maximum temperature differential to control cracking in massive concrete applications should be supplemented with a requirement for the presentation of a finite element analysis showing the calculated stress response to the predicted temperature distribution within the concrete, to ensure that the induced tensile stresses will not exceed the tensile strength of the concrete.

References

Ballim, Y. and P. J. F. s. C. T. Graham (2009). "Thermal properties of concrete and temperature development at early ages in large concrete elements."

Brown, T. and M. J. M. e. C. Javaid (1970). "The thermal conductivity of fresh concrete." **3**(6): 411-416.

Campbell-Allen, D. and C. Thorne (1963). "The thermal conductivity of concrete." <u>Magazine of concrete Research</u> **15**(43): 39-48.

Cervera, M., et al. (2000). "Simulation of construction of RCC dams. II: stress and damage." **126**(9): 1062-1069.

Choktaweekarn, P., et al. (2009). "A model for predicting thermal conductivity of concrete." **61**(4): 271-280.

Committee, A. (2005). <u>Building code requirements for structural concrete (ACI 318-05)</u> and commentary (ACI 318R-05), American Concrete Institute.

Conrad, M. (2006). <u>A contribution to the thermal stress behaviour of Roller-Compacted-Concrete (RCC) gravity dams-field and numerical investigations</u>, Techn. Univ., Lehrstuhl für Wasserbau und Wasserwirtschaft im Inst. für

De Schutter, G. J. C. and Structures (2002). "Finite element simulation of thermal cracking in massive hardening concrete elements using degree of hydration based material laws." **80**(27-30): 2035-2042.

FitzGibbon, M. and F. ME (1976). "LARGE POURS. II. HEAT GENERATION AND CONTROL."

Gajda, J. (2007). Mass concrete for buildings and bridges.

Ghosh, S. (1991). <u>Cement and concrete science and technology</u>. 1, 1, Thomas Telford.

Hansen, P., et al. (1982). "THERMAL PROPERTIE OF HARDENING CEMENTPASTE."

Khan, M. J. B. and Environment (2002). "Factors affecting the thermal properties of concrete and applicability of its prediction models." **37**(6): 607-614.

Kim, K.-H., et al. (2003). "An experimental study on thermal conductivity of concrete." **33**(3): 363-371.

Kodur, V., et al. (2012). "Structures in fire: state-of-the-art, research and training needs." **48**(4): 825-839.

Law, A., et al. (2011). "Structural engineering and fire dynamics: advances at the interface." **10**: 1563-1576.

Lawrence, A. M. (2009). <u>A finite element model for the prediction of thermal</u> stresses in mass concrete.

Maréchal, J. J. C. t. t. T. G. W. (1973). "Determination simultanée de la diffusivité et de la conductivité thermique du beton pendant son hydration." **40**.

Mehta, P. K. and P. J. Monteiro (2017). <u>Concrete microstructure</u>, <u>properties and materials</u>.

R-07, A. C. I. J. A. (2007). Report on thermal and volume change effects on cracking of mass concrete.

RILEM, T. J. M. and Structures "42-CEA. 1981. Properties of Set Concrete at Early Ages: State of the Art Report." **14**(84): 399-450.

Saul, A. J. M. o. C. R. (1951). "Principles underlying the steam curing of concrete at atmospheric pressure." **2**(6): 127-140.

Tatro, S. and E. Schrader (1992). <u>Thermal analysis for RCC—a practical approach</u>. Roller compacted concrete III, ASCE.

Tia, M., et al. (2010). Development of design parameters for mass concrete using finite element analysis: final report, February 2010, Florida. Dept. of Transportation.

White, G. R. (1977). Concrete technology, Van Nostrand Reinhold Company.

Zhu, B. J. J. o. c. e. and management (1999). "Effect of cooling by water flowing in nonmetal pipes embedded in mass concrete." **125**(1): 61-68.